

## Supplementary Information

### Catalyst activity or stability: the dilemma in Pd-catalyzed polyketone synthesis

Francesco Amoroso,<sup>a,b</sup> Ennio Zangrando,<sup>a</sup> Carla Carfagna,<sup>c</sup> Christian Müller,<sup>d</sup> Dieter Vogt,<sup>e</sup> Mohamed Hagar,<sup>f</sup> Fabio Ragagni,<sup>\*g</sup> and Barbara Milani<sup>\*a</sup>

<sup>a</sup> Dipartimento di Scienze Chimiche e Farmaceutiche, Università di Trieste, Via Licio Giorgieri 1, 34127 Trieste, Italy. Fax: 39 040 5583903; Tel: 39 040 5583956; E-mail: milaniba@units.it

<sup>b</sup> Dipartimento di Chimica, Fisica e Ambiente, Università di Udine, Via del Cotonificio 108, 33100 Udine, Italy. Fax: 0432 558803; Tel: 0432 558755; e-mail: francesco.amoroso@uniud.it

<sup>c</sup> Dipartimento di Scienze Biomolecolari, Università di Urbino, Piazza Rinascimento 6, 61029 Urbino, Italy. Fax: 39 0722 303311; Tel: +39 0722 303312; E-mail: carla.carfagna@uniurb.it

<sup>d</sup> Institut für Chemie und Biochemie-Anorganische Chemie, Freie Universität Berlin, 14195 Berlin, Germany. Tel: +49 30 838 54004; e-mail: c.mueller@fu-berlin.de

<sup>e</sup> School of Chemistry, University of Edinburgh, Edinburgh EH9 3JJ, Scotland, UK. Tel: +44 131 651 7767; e-mail: d.vogt@ed.ac.uk

<sup>f</sup> Chemistry Department, Alexandria University, Ibrahimia, Alexandria 21321, Egypt.

<sup>g</sup> Dipartimento di Chimica, Università di Milano, Via C. Golgi 19, 20133 Milano, Italy; Fax: 02 50314405; Tel: 02 50314373; E-mail: fabio.ragagni@unimi.it.

#### Table of content

	Page
General discussion on the fitting procedure	S2
Copies of NMR spectra	S34

## General discussion on the fitting procedure

### Data collection and experimental artifacts

The apparatus employed for the determination of the reaction rate is operated along the following main lines:

- 1) The apparatus is inertized with argon and the reagents and solvents are added to the autoclave by a side port. The autoclave is then filled with CO at the desired pressure at room temperature.
- 2) At this stage heating is started. When the autoclave reaches the set temperature (30 °C for all experiments), gas consumption starts to be measured ( $t = 0$ ).
- 3) Gas consumption is measured by an integrated flow meter. Pressure inside the autoclave is checked at set time intervals and if the value differs from the set value by more than 0.5 bar, CO is added until the set pressure is reached in the autoclave.

This kind of procedure causes two experimental artifacts.

- 1) The reaction starts immediately when CO is charged at room temperature and proceeds to some extent before the set temperature is reached. This results in some CO consumption (pressure drop) before measurement is started. On the other hand, the raise in temperature causes an increase in the internal pressure of the autoclave and this can lead it to override the set value (pressure increase). The two effects tend to counterbalance each other, but do not necessarily do this completely. If the reaction is initially very fast, the pressure drop will prevail. Thus when the set temperature is reached the instruments will suddenly restore the pressure and a sharp vertical CO absorption will be detected. On the other hand, if the reaction is slow, the pressure increase will prevail. Under these conditions, at  $t = 0$  no CO is added and none is so until the reaction proceeds to the point that the set pressure is reached again. This results in an apparent induction period, from which, however, the reaction exits in a sharp way, rather than smoothly as commonly observed. As a matter of facts, both behaviors were observed in some cases. The first was clearly detected only in one case (for a reaction run under 10 bar CO that had anyway to be discarded because of excessive noise in the line), whereas the second was always observed when the reactions were performed under 3 bar CO. In the worse case, no CO absorption was measured for about 50 min. Fortunately, the phenomenon was less evident for the reactions run under 5 bar CO, which however simply means the two effects are compensating each other, not that they are not occurring.

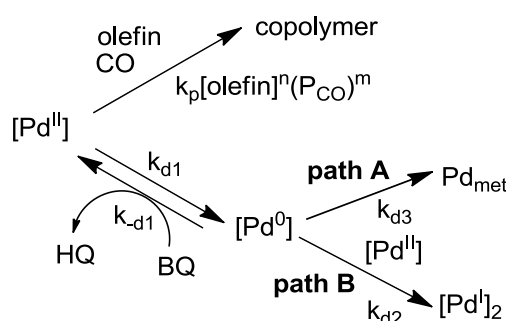
2) The type of pressure adjustment described above results in a series of steps in the gas consumption vs. time plots, which are especially evident in the first part of the plot, when reaction rate is higher. Although these steps are often not evident if the plot is observed at a low magnification, they result in the derivative of the plot having sudden variations from zero to extremely high values, making a derivative plot completely meaningless. We will return on this point later.

### Fitting procedures for the kinetic data by integration of different rate laws

A general reaction pathway evidencing the catalyst decomposition is shown in Scheme 1. A palladium(II) species catalyzes the copolymerization reaction with a kinetic constant  $k_p$  (the kinetic order with respect to the reagents has been left unspecified for the moment). Since the olefin is present in large excess and CO is continuously replenished, the concentration of both reagents is constant during the reaction and the rate is only dependent on the active palladium concentration, which decreases with time because of catalyst decomposition:

$$\text{rate} = k_1[\text{Pd}^{\text{II}}] \quad (1)$$

where  $k_1$  is the apparent first order kinetic constant with respect to the active catalyst concentration. Note that rigorously speaking,  $[\text{Pd}^{\text{II}}]$  should be the concentration of the palladium complex involved in the r.d.s. of the reaction (whichever it is), but this can be considered to be very close to the total concentration of palladium(II) species in solution.



Scheme 1

Experimentally, the actual reaction rate is measured by the CO consumption (mmol/h), but in order to have the kinetic constants expressed in the usual units ((time unit)<sup>-1</sup> for first order kinetics)

it is better to divide the CO absorption (in mmol) by the reaction solution volume ( $V = 8$  mL for all reactions). That is:

$$\text{rate} = d[(\text{CO abs}/\text{mmol})/(V/\text{mL})]/dt = k_p[\text{Pd}^{\text{II}}][\text{olefin}]^n(P_{\text{CO}})^m = k_1[\text{Pd}^{\text{II}}] \quad (2)$$

where  $[\text{Pd}^{\text{II}}]$  depends on time.

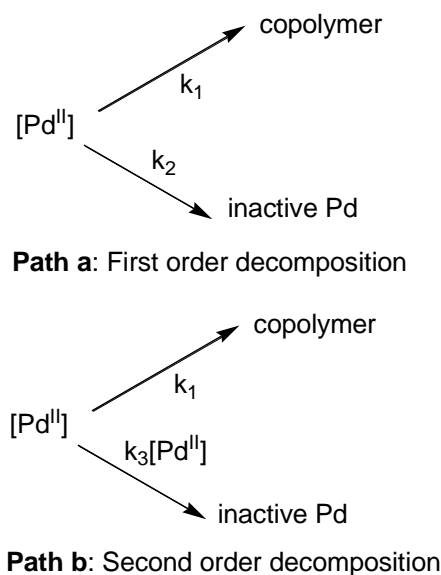
As far as catalyst decomposition is concerned, it is well recognized that in the present catalytic system this is due to palladium(II) reduction, as also indicated by the fact that benzoquinone retards such deactivation by oxidizing back the palladium(0) complex (processes associated to  $k_{d1}$  and  $k_{-d1}$  in Scheme 1) and that metallic palladium is observed sometimes after complete catalyst deactivation. There is little doubt that the initial step for decomposition is reduction of a single palladium(II) complex to palladium(0). Although several possibilities exists for such a process, it is almost surely described by a first order kinetics with respect to palladium(II). What it occurs later is less obvious. Several papers have been devoted to the kinetics of metallic nanoparticles formation, but they usually focus on later stages of the reaction.<sup>1,2</sup> As far the early stages of decomposition are concerned, we can identify two general reaction pathways.

In the first pathway (path A in Scheme 1), the palladium(0) complex decomposes by an irreversible unimolecular pathway, *e.g.* an irreversible loss of the nitrogen ligand, to eventually give metallic palladium. Alternatively, the palladium(0) complex can react with a palladium(II) complex to afford an inactive palladium(I) dimer (path B). Precedents exist for such a process.<sup>3-5</sup> Very recently some of us identified a series of complexes of general structure  $[\text{Pd}^{\text{I}}\text{L}^2\text{X}(\mu\text{-CO})]_2$  ( $\text{L}_2 = \text{phen, bpy or their substituted analogues, X = halide, carboxylate, -C(O)OCH}_3$ ) as intermediates in the reduction of palladium(II) complexes by CO and water or alcohols under conditions close to those employed in the presently studied system<sup>6</sup> and the formation of the corresponding Ar-BIAN complexes may as well occur easily.

The possibility that the irreversible step of the decomposition is the reaction of two palladium(0) complexes should also be considered. However, palladium(0) complexes concentration should be very low at any moment and this process is quite unlikely to play a relevant role in the present system. From a kinetic point of view, a process of this kind would be distinguishable from that in path B only if the concentration/time profile for benzoquinone were also known, which is not the case, and so we will ignore it in the following.

Modeling the complete system without knowing the benzoquinone concentration *vs.* time profile is not possible in general, even if the steady state approximation is applied to the Pd(0) complex. However, in those cases in which deactivation is limited, it can be approximated that benzoquinone

concentration is essentially constant during the reaction. Under these conditions paths a and b can be respectively described approximately by a first and a second kinetics with respect palladium(II) concentration (Scheme 2).



**Scheme 2**

The first order decomposition is described by equations 3 and 4:

$$d[Pd^{II}]/dt = -k_2[Pd^{II}] \quad (3)$$

$$[Pd^{II}]_t = [Pd^{II}]_0 e^{-k_2 t} \quad (4)$$

Where  $[Pd^{II}]_0$  and  $[Pd^{II}]_t$  are the palladium(II) concentrations at time zero and  $t$  respectively.

From eqs. 4 and 2, eq. 5 is derived, which leads to eq. 6 after integration.

$$\text{rate} = d[(CO \text{ abs})/V]/dt = k_1[Pd^{II}]_0 e^{-k_2 t} \quad (5)$$

$$(CO \text{ abs})/V = (k_1/k_2)[Pd^{II}]_0(1 - e^{-k_2 t}) \quad (6)$$

where  $[Pd^{II}]_0 = 1.32 \times 10^{-4}$  M. Note that using this value for  $[Pd^{II}]_0$  is an approximation because the reaction and the deactivation start effectively before time zero for the data collection. However, if deactivation is small, the difference may be negligible.

Equation 6 is of the type  $Y = a(1 - e^{-bX})$ , a Stirling type function, and can be modeled by a suitably modified fitting function in the program Origin, to give the best  $a$  and  $b$  values, from which  $k_1$  and  $k_2$  are immediately calculated.

For the second order decomposition pathway, an analogous procedure leads to the equations:

$$d[Pd^{II}]/dt = -k_3[Pd^{II}]^2 \quad (7)$$

$$[Pd^{II}]_t = [Pd^{II}]_0 / (1 + k_3[Pd^{II}]_0 t) \quad (8)$$

$$\text{rate} = d[(\text{CO abs})/V]/dt = k_1[\text{Pd}^{\text{II}}]_0/(1+k_3[\text{Pd}^{\text{II}}]_0 t) \quad (9)$$

$$(\text{CO abs})/V = (k_1/k_3)\ln(1+k_3[\text{Pd}^{\text{II}}]_0 t) \quad (10)$$

Equation 10 corresponds to a logarithmic function that can again be modeled in Origin.

### Fitting by integration of the 4-methylstyrene experiments run under 5 bar CO

The most extensive series of experiments both with styrene and 4-methylstyrene were run under 5 bar CO and at mol ratio benzoquinone/Pd = 5. Since deactivation was clearly lower with the latter substrate, we will start analyzing the corresponding set of data. A plot of all CO absorption *vs.* time for this set of experiments is shown in Figure S1.

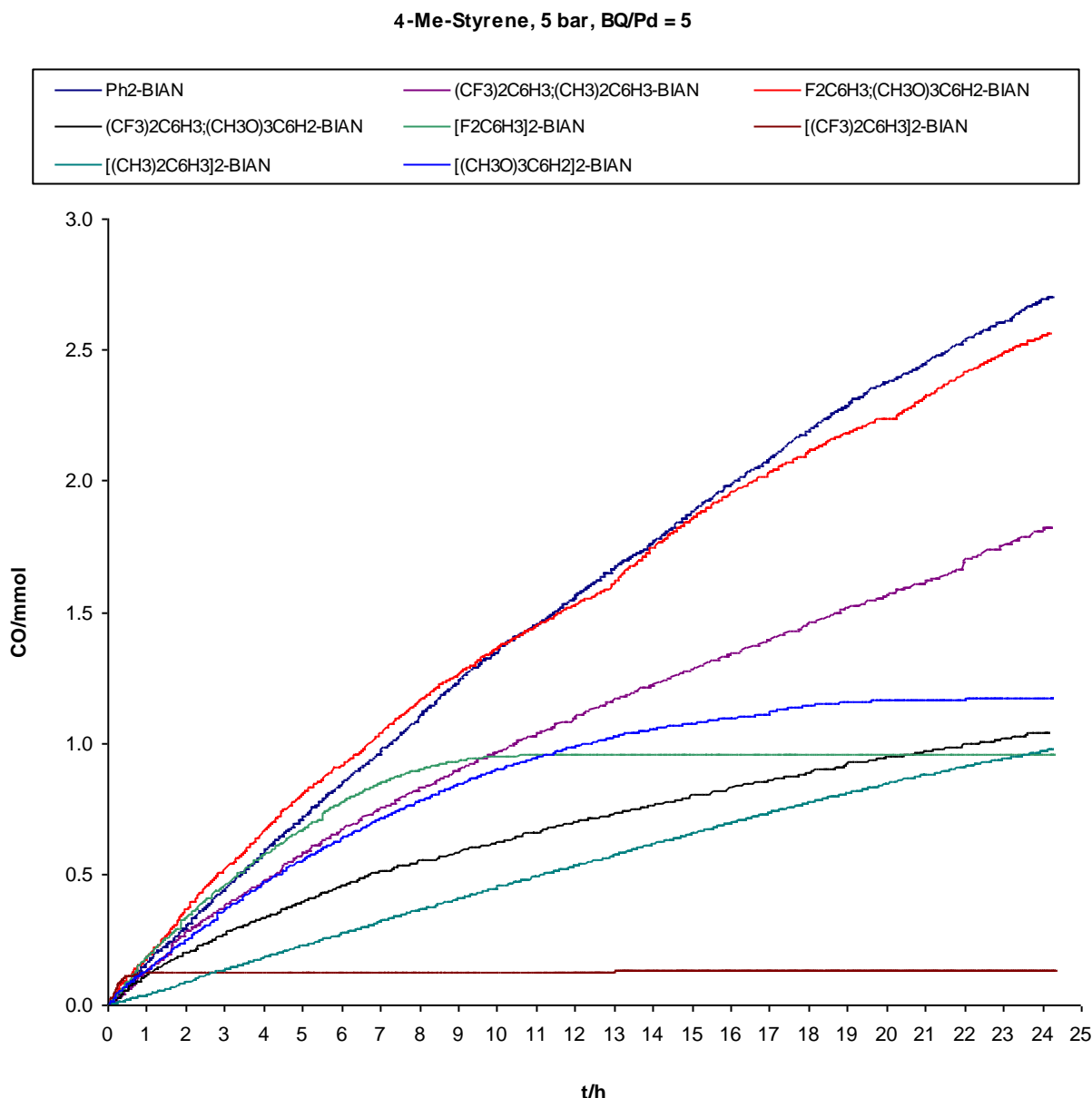


**Figure S1.** CO absorption plots for the copolymerization of 4-methylstyrene under 5 bar CO ( $[BQ]/[Pd] = 5$ ) catalyzed by different  $[Pd(CH_3)(CH_3CN)(Ar-BIAN)][PF_6]$  complexes.

We attempted modeling all the kinetic plots by both models. However, it was immediately recognized that whereas excellent results could be obtained in most cases when eq. 10 (path b; second order decomposition) was employed, eq. 6 (path a; first order decomposition) only afforded a good fit in those two cases (Ph<sub>2</sub>-BIAN, [3,5-(CH<sub>3</sub>)<sub>2</sub>C<sub>6</sub>H<sub>3</sub>]<sub>2</sub>-BIAN) in which decomposition is so limited that basically any model would successfully fit it.

As an example, the comparison of the fit obtained for the same set of data by the two models is shown in Figure S2, where the data for the experiment using 3,5-(CF<sub>3</sub>)<sub>2</sub>C<sub>6</sub>H<sub>3</sub>;3,4,5-(CH<sub>3</sub>O)<sub>3</sub>C<sub>6</sub>H<sub>2</sub>-

BIAN are shown together with the respective fitting lines. Note that since the reaction volume is constant, fitting was always performed on the original CO absorption data in mmol and division by the reaction value was done later.

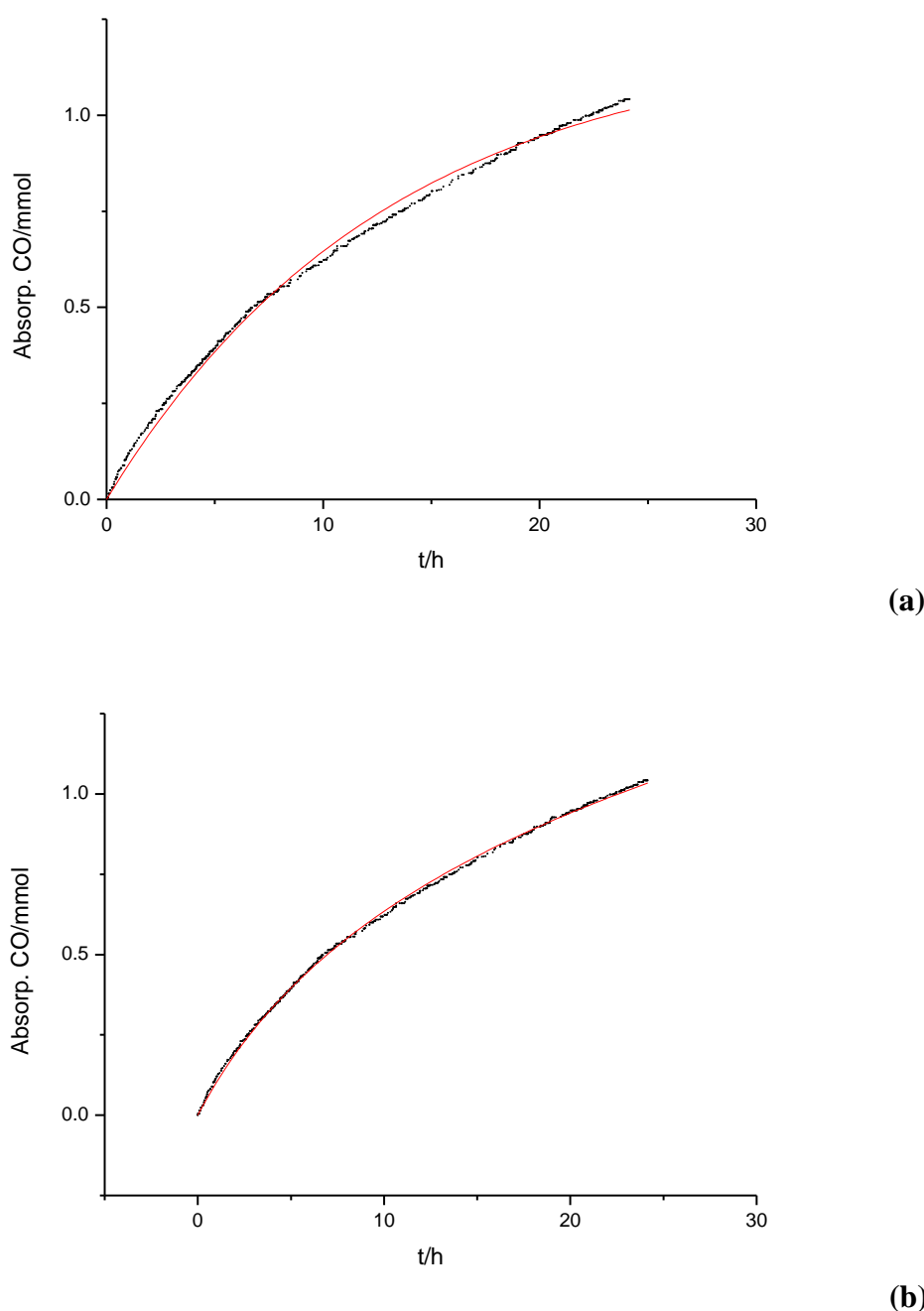


**Figure S2.** Data for the copolymerization of 4-methylstyrene under 5 bar CO ( $[BQ]/[Pd] = 5$ ) and with  $3,5-(CF_3)_2C_6H_3;3,4,5-(CH_3O)_3C_6H_2$ -BIAN as a ligand. (a) Fitting by eq. 6 (first order decomposition). (b) Fitting by eq. 10 (second order decomposition).

Even from a quick examination of Figure S2 it is clear that eq. 10 fits very well the data in the whole time region, whereas eq. 6 tends to underestimate catalyst decomposition (which is proportional to the second derivative of the CO absorption plot; see later) at the beginning of the reaction and to overestimate it later. The initial underestimation is especially significant. In fact, if the assumption that benzoquinone concentration is approximately constant was wrong, then catalyst decomposition should be slower than calculated during the first part of the reaction, when benzoquinone is more abundant. This would result in the model giving an even worse fitting of the data and cannot justify the observed discrepancies. Thus it is clear that the process associated with path a must be discarded as a relevant deactivation mode for palladium, whereas the goodness of the fit obtained by modeling path b strongly supports its operation. It is worth of note that such a good fit was obtained with only two floating parameters, which would be unlikely to occur if the physical basis of the model were wrong.

Equation 10 could be used to fit the data of five of the reaction profiles with an excellent approximation (adj.  $R^2 > 0.999$ ), but gave significant deviations in the remaining three cases ( $[3,5-F_2C_6H_3]_2$ -BIAN,  $[3,5-(CF_3)_2C_6H_3]_2$ -BIAN,  $[3,4,5-(CH_3O)_3C_6H_2]_2$ -BIAN), where catalyst decomposition is more evident and the assumption that benzoquinone concentration does not vary is clearly untenable. We will discuss here these five cases. The values of  $k_1$  and  $k_3$  best fitting the data are reported in Table S1. In previous papers some of us have shown that the logarithm of the relative coordinating strength of substituted Ar-BIAN ligands shows a good correlation with the Hammett  $\sigma$  constants.<sup>7,8</sup> When two substituents were present, the correlation was maintained if the sum of the two individual  $\sigma$  was employed, whereas ligands having different substituents on the two aryl rings followed the same trend if the arithmetic average of the Hammett  $\sigma$  constants for the two rings was employed in the correlation.<sup>9</sup> In general, this corresponds to employing for both symmetrical and nonsymmetrical ligands the value  $\Sigma\sigma/2$  (where the sum is extended to all substituents on the two rings) and this value is also shown in the table.

**Table S1:** Fitting of five reactions run with 4-methylstyrene under 5 bar CO ( $[BQ]/[Pd] = 5$ ) by equation 10.

Ligand	$\Sigma\sigma/2$	$k_1/h^{-1}$	$k_3/h^{-1}M^{-1}$
$[3,5-(CH_3)_2C_6H_3]_2$ -BIAN	-0.14	46	127
Ph <sub>2</sub> -BIAN	0	149	279
3,5-F <sub>2</sub> C <sub>6</sub> H <sub>3</sub> ;3,4,5-(CH <sub>3</sub> O) <sub>3</sub> C <sub>6</sub> H <sub>2</sub> -BIAN	0.325	173	548
3,5-(CH <sub>3</sub> ) <sub>2</sub> C <sub>6</sub> H <sub>3</sub> ;3,5-(CF <sub>3</sub> ) <sub>2</sub> C <sub>6</sub> H <sub>3</sub> -BIAN	0.36	125	609
3,5-(CF <sub>3</sub> ) <sub>2</sub> C <sub>6</sub> H <sub>3</sub> ;3,4,5-(CH <sub>3</sub> O) <sub>3</sub> C <sub>6</sub> H <sub>2</sub> -BIAN	0.415	105	1364

Logarithmic plots of  $k_1$  and  $k_3$  with respect to  $\Sigma\sigma/2$  are shown in Figures S3 and S4. Note that a shortened notation for the ligand names is given close to each data point, only mentioning the substituents on the ligand.

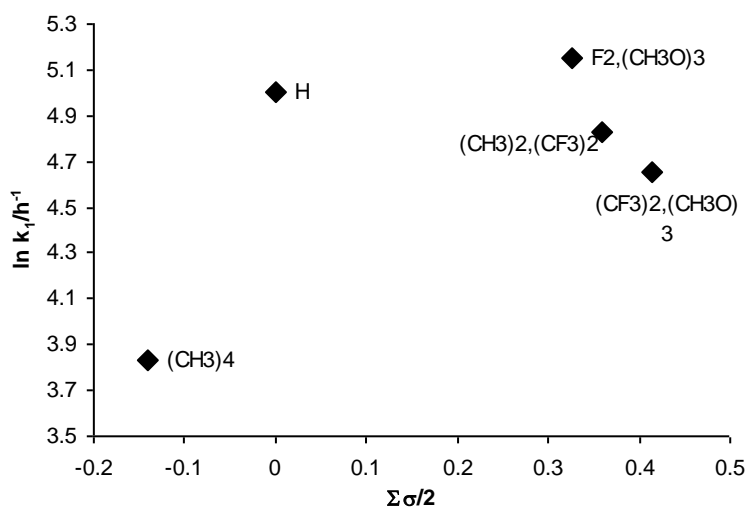


Figure S3

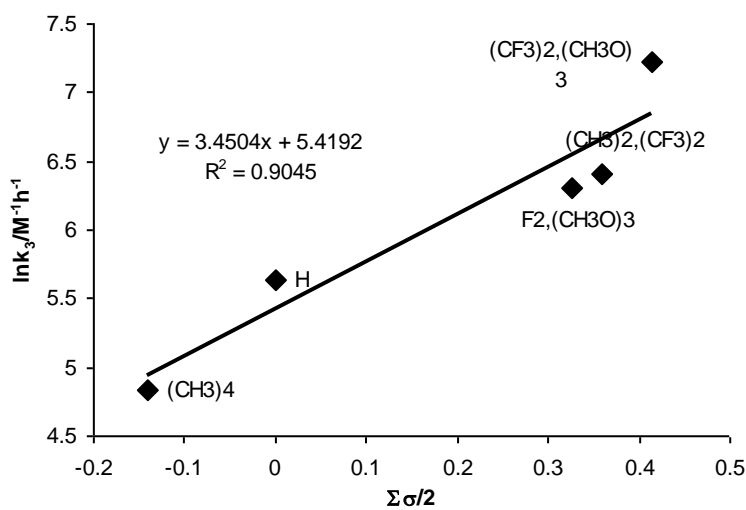


Figure S4

From the plots it is evident that the presence of electron-withdrawing substituents leads to catalytic systems that deactivates at a faster rate (higher  $k_3$  values) and an approximately linear correlation with  $\Sigma\sigma/2$  exists (Figure S4). A correlation between  $\Sigma\sigma/2$  and the reaction rate is less

evident. In general it appears that electron-withdrawing groups lead to more active systems, but the ligands having hydrogen or fluorine as substituents give more active systems than expected, suggesting that steric hindrance even in the *meta* position disfavors the catalytic reaction. The validity of this trend is however limited by the number of data points.

#### **Fitting of the 4-methylstyrene experiments run under 5 bar CO by interpolation of the original data, differentiation and analysis of the first and second differential plots**

In order to obtain some information even from the reactions that could not be fit by eq. 10, a different approach was followed. Indeed, some information can be gained by noting that:

1) Since the CO pressure is kept constant and the olefin concentration is high enough that it can be considered constant during the reaction (pseudo zero order kinetics with respect to both CO and olefin), then the reaction rate is proportional only to the active palladium concentration. The reaction rate as a function of time can in theory be obtained by differentiating the CO absorption curve. Thus eq. 2 can be rearranged to give eq. 11,

$$[\text{Pd}^{\text{II}}] = (d[(\text{CO abs}/\text{mmol})/(\text{V}/\text{mL})]/dt)/k_1 \quad (11)$$

which describes the time evolution of the Pd(II) concentration in solution. In eq. 11,  $k_1$  represents the pseudo first order (with respect to palladium) constant for the copolymerization reaction. If  $k_1$  were available, the complete kinetic constant could be easily calculated by dividing  $k_1$  for the olefin concentration and CO pressure, which are known and constant throughout the reaction.

2) Given what said above, the opposite of the derivative of the  $[\text{Pd}(\text{II})]$  with respect to time is the rate of decomposition of the catalytic system.

$$\text{catalyst decomposition rate} = -d[\text{Pd}^{\text{II}}]/dt \quad (12)$$

The latter is proportional to the opposite of the second derivative of the CO absorption vs. time curve. It is important to stress that the two are just proportional and not the same because of the presence of  $k_1$ . By differentiating eq. 2 and substituting eq. 12 in the resulting equation, we get:

$$-d^2[(\text{CO abs}/\text{mmol})/(\text{V}/\text{mL})]/dt^2 = -k_1(d[\text{Pd}^{\text{II}}]/dt) = k_1 \cdot (\text{catalyst decomposition rate}) \quad (13)$$

Since  $k_1$  is different for each reaction, a direct comparison must be made with caution. However, if a reasonable estimation of  $k_1$  can be given, then a quantitative comparison becomes possible. This constant is connected to the first derivative plot by eq. 2. By substituting the  $k_1$  value from the latter equation into eq. 13 and simplifying the reaction volume, eq. 14 is obtained.

$$\text{catalyst decomposition rate} = -d[\text{Pd}^{\text{II}}]/dt = -[\text{Pd}^{\text{II}}][d^2(\text{CO abs})/dt^2]/[d(\text{CO abs})/dt] \quad (14)$$

Note that eqs. 13 and 14 hold whichever is the catalyst decomposition kinetics and that the “catalyst decomposition rate” indicated is a curve and not a constant. However, since the actual  $[\text{Pd}^{\text{II}}]$  value at any time is not known and is again different for each reaction, a comparison can only be made at time zero, assuming that any catalyst decomposition is negligible (this is an approximation, as discussed above) and that reliable values for the first and second derivative of the CO absorption plot at this time can be given. In specific cases, more information may be gained. For example, if eq. 7 holds, then  $k_3$  can be determined, as we will detail later.

Differentiating two times the CO abs. curve is apparently simple to do, but we must recall the problems mentioned before (point 2 in the list of the artifacts), that is the original data show numerous “steps” and this results in the first derivative of CO abs. vs. t plot to suddenly jump from 0 to extremely high values very often, making any analysis of the resulting plot or its further differentiation completely meaningless. To solve this problem the following strategy was devised:

1) First a suitable fitting function was identified that is able to fit very well the original data, independent of any associated physical meaning. Among the (numerous) functions predefined in Origin 8.0, we found that exponentials decays are best suited and very good results were obtained by using a three terms exponential decay function (ExpDec3). The general form of the fitting function is:

$$Y = a e^{-X/b} + c e^{-X/d} + f e^{-X/g} + h \quad (15)$$

Despite the fact that no physical meaning can be attributed to the optimized parameters, excellent fits could be obtained by applying this function to the original data. The adj. $R^2$  value was higher than 0.999 in almost every case. A very high sampling frequency (1500 points for the whole kinetics) was applied in the interpolation not to lose precision with respect to the original data (about 1650 points for each analysis). It should be mentioned that a triple exponential function as

that employed is not strictly necessary for all kinetic runs. In many cases a strong correlation between some parameters was observed and a double exponential function would have given comparable results. However, we preferred to use always the same function not to risk to introduce any difference in the mathematical treatment of different runs.

As an example, the original data points for the experiment employing the symmetrical ligand with four trifluoromethyl groups,  $[3,5-(CF_3)_2C_6H_3]_2\text{-BIAN}$ , and the corresponding fitting curve calculated by eq. 15 are shown in Figure S5. This is the reaction whose data gave the worse fitting by eq. 10. This is not surprising since it is apparent at first glance that a marked bending of the CO absorption *vs.* time curve is present and this clearly indicates that the assumption that catalyst decomposition is limited is untenable for this reaction. Yet eq. 15 fits the data very well (Adj.  $R^2 = 0.9992$ ) despite the fact that the optimized coefficients have no physical meaning.

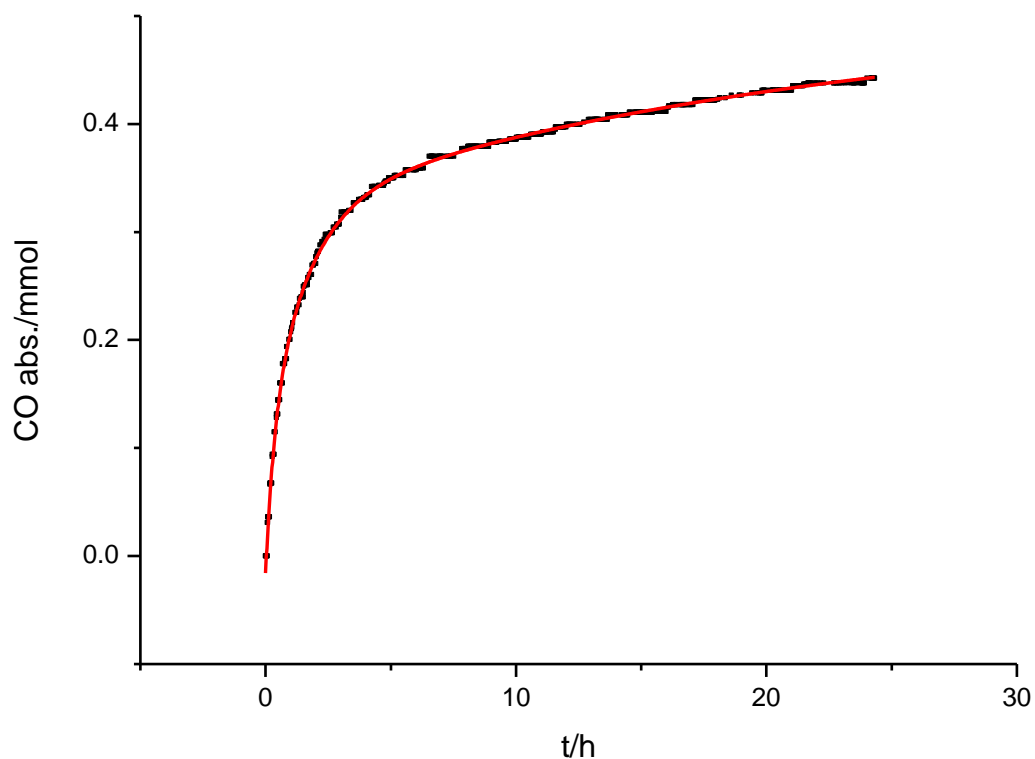


**Figure S5.** Original data and fitting function calculated by eq. 15 for the copolymerization reaction of 4-methylstyrene and CO (5 bar) catalyzed by  $[\text{Pd}(\mathbf{5})(\text{CH}_3)(\text{CH}_3\text{CN})][\text{PF}_6]$  ( $[\text{BQ}]/[\text{Pd}] = 5$ ).

2) At this stage the interpolated function, not the original data, was differentiated two times (by using the Origin 8.0 built-in routine). Since the interpolating function is smooth, the previously mentioned problems were not encountered. The only remaining problem is with the value of the

second derivative during the first few minutes after the starting of the reading by the instrument. In general, the opposite of the second derivative is a smoothly decreasing function through the overwhelmingly majority of the reaction, but very often a sudden increase was observed in the first few minutes. This is clearly a mathematical artifact in the differentiation procedure and has no physical meanings. However, its presence prevented us from employing the value of the second derivative at time zero as a significant value. The value after 2 minutes was taken instead, since all runs showed a regular behavior at this point. The difference between this value and the apparent value at time zero obtained by extrapolating the smooth part of the derivative plot is anyway negligible and we did not introduce any further mathematical elaboration to better estimate this value. The plots of the first or second derivative for different reactions can be overlapped and compared or be further analyzed.

3) In general the largest residuals in the fitting procedures were obtained for the first reaction minutes. This is unfortunate, because the corresponding data may be very useful. In order to have a better estimate of the first derivative at time zero we fitted the original data to only the first reaction hour. In this case a very close agreement between experimental and simulated plots was obtained even for the initial reaction minutes. However, the curve deriving from the fit of all the data was employed to calculate the second derivative, because in this case the shape of the curve is more important than the original intercept value and this is better defined by a larger data set.

The aforementioned calculations were performed for all the kinetic runs in the series. Plots of the first and second derivative of CO absorption are shown in figures S6 and S7.

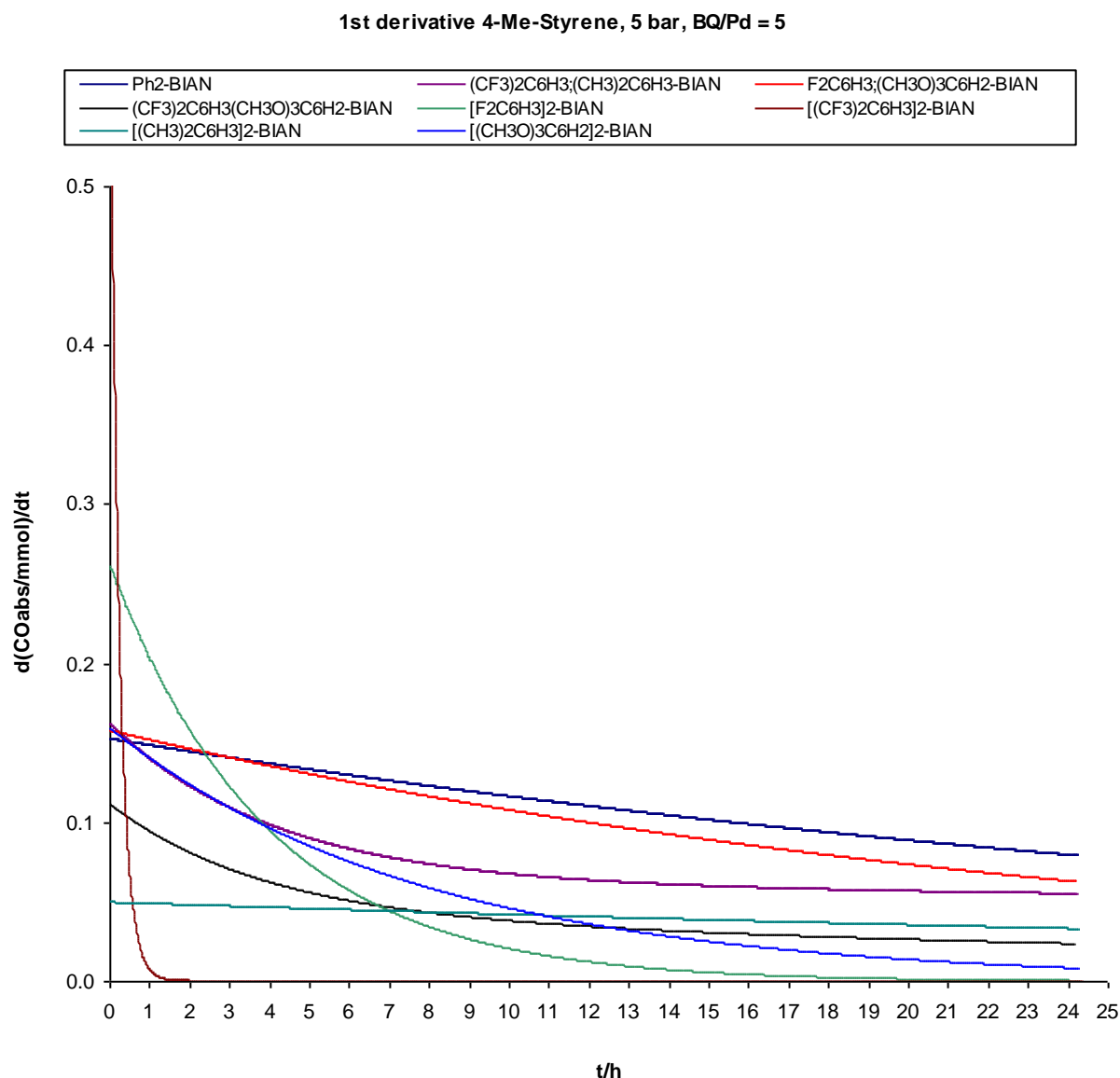


**Figure S6.**

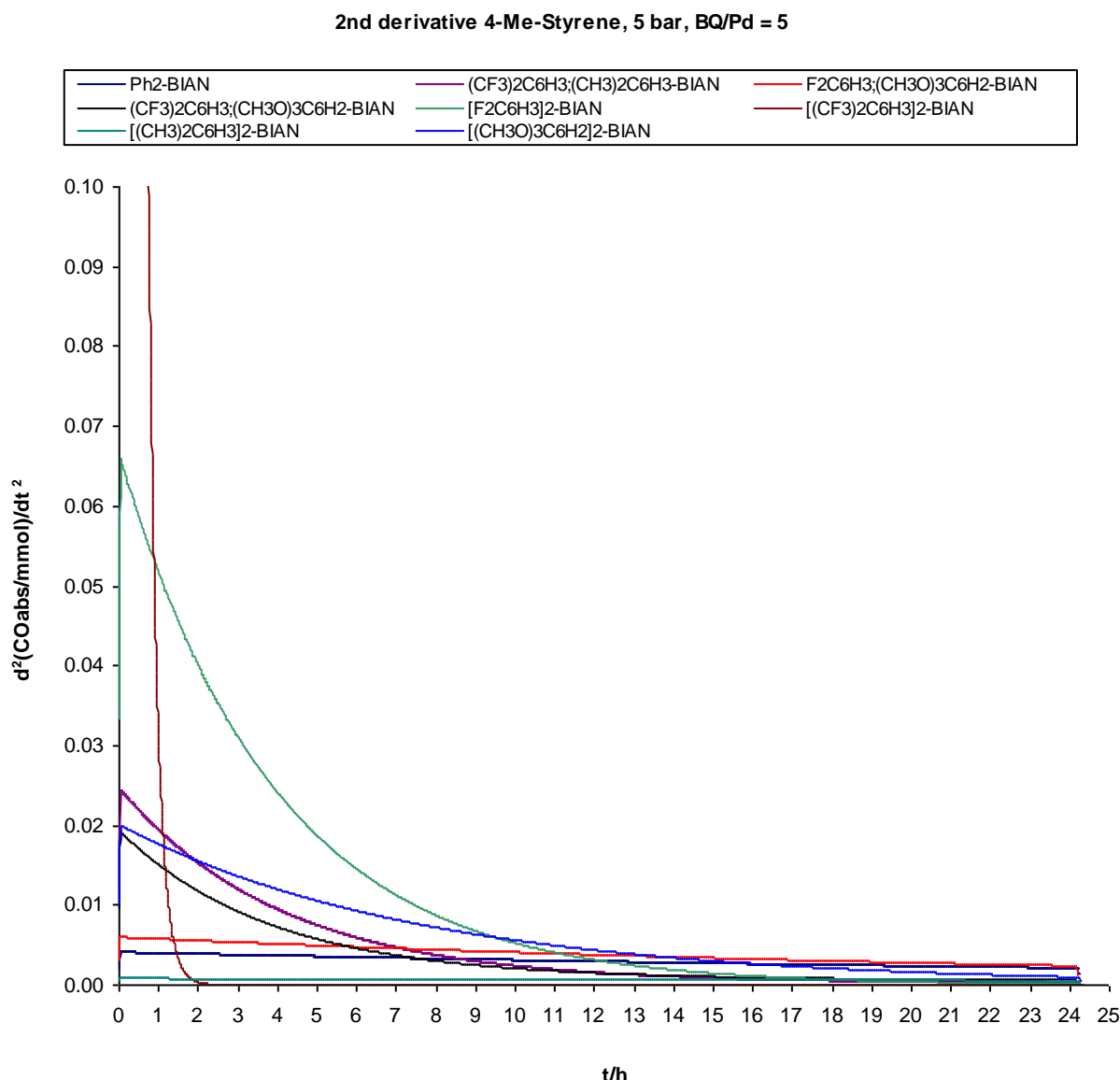


**Figure S7**

Even a qualitative inspection of figures S6 and S7 reveals that the previously evidenced tendency of more active systems to deactivate more quickly is followed even when the three additional ligands are added. Moreover, the tetrafluoro- and the tetra(trifluoromethyl)-substituted ligands also fit the general rule that electron-withdrawing substituents gives more active systems. The activity and deactivation rates of the latter ligand are striking. Although on a long timescale  $[3,5-(CF_3)_2C_6H_3]_2\text{-BIAN}$  gave the worse conversion (see Figure S1), from Figure S6 it appears that at short reaction times it affords by far the more active catalytic system, although the corresponding deactivation rate is also extremely high.

In order to get a more quantitative comparison, we must consider what said before. From eq. 2, the derivative plot (of the CO absorption curve) gives the value  $k_1[Pd^{II}]V$  at any time. The palladium(II) concentration is not known at any time, but if we assume that at time zero decomposition has not started yet, we can calculate  $k_1$  from the value of the derivative plot at this time and the initial palladium concentration:

$$k_1' = (d(CO\ abs)/dt)_0 / ([Pd^{II}]_0 V) \quad (16)$$

We named the value calculated in this way  $k_1'$  to distinguish it from that calculated by the fitting procedure described in the previous paragraph, although  $k_1$  and  $k_1'$  should ideally be the same.

Values of  $k_1'$  calculated by eq. 16 using the  $(d(CO\ abs)/dt)_0$  value derived from the first derivative plots for all reactions run with 4-methylstyrene under 5 bar CO and with a mol ratio  $BQ/Pd = 5$  are reported in Table S2 (we recall that we used the function interpolated to only the first reaction hour for this purpose instead of that for the complete reaction shown in Figure S6). A comparison between these values and the corresponding  $k_1$  values for corresponding reactions (when available) reported in Table S1 shows that the agreement is excellent in three out of five cases ( $[3,5-(CH_3)_2C_6H_3]_2$ -BIAN:  $k_1 = 46$ ,  $k_1' = 45$ ;  $Ph_2$ -BIAN:  $k_1 = 149$ ,  $k_1' = 144$ ;  $3,5-(CH_3)_2C_6H_3;3,5-(CF_3)_2C_6H_3$ -BIAN:  $k_1 = 125$ ,  $k_1' = 123$ ), but it is acceptable even for the other two, thus validating the mathematical approach employed.

**Table S2:** Values of  $k_1'$  and  $k_3'$  calculated from eqs. 16 and 19 for of all reactions run with 4-methylstyrene under 5 bar CO ( $[BQ]/[Pd] = 5$ ).

Ligand	$\Sigma\sigma/2$	$k_1'/h^{-1}$	$k_3'/h^{-1}M^{-1}$
$[3,5-(CH_3)_2C_6H_3]_2$ -BIAN	-0.14	45	$1.33 \times 10^2$
$[3,4,5-(CH_3O)_3C_6H_2]_2$ -BIAN	-0.03	182	$7.85 \times 10^2$
$Ph_2$ -BIAN	0	144	$2.05 \times 10^2$
$3,5-F_2C_6H_3;3,4,5-(CH_3O)_3C_6H_2$ -BIAN	0.325	151	$2.85 \times 10^2$
$3,5-(CH_3)_2C_6H_3;3,5-(CF_3)_2C_6H_3$ -BIAN	0.36	123	$1.40 \times 10^3$
$3,5-(CF_3)_2C_6H_3;3,4,5-(CH_3O)_3C_6H_2$ -BIAN	0.415	122	$1.12 \times 10^3$
$[3,5-F_2C_6H_3]_2$ -BIAN	0.68	188	$2.51 \times 10^3$
$[3,5-(CF_3)_2C_6H_3]_2$ -BIAN	0.86	553	$3.35 \times 10^4$

A logarithmic plot of  $k_1'$  vs.  $\Sigma\sigma/2$  analogous to that shown in Figure S3 for  $k_1$  is shown in Figure S8.

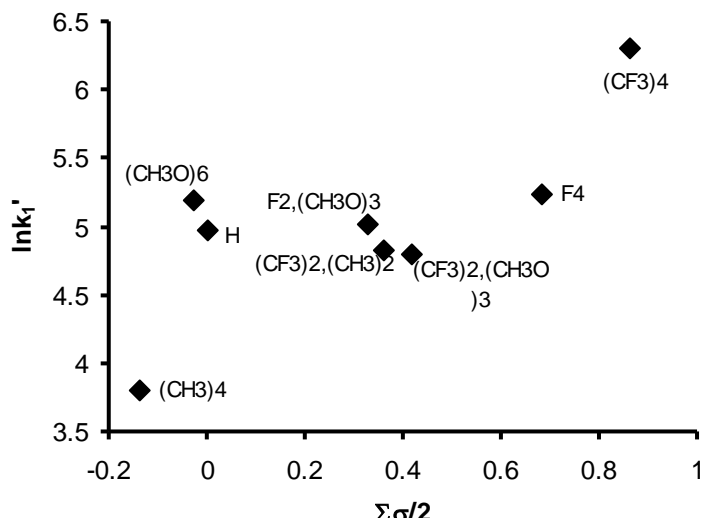


**Figure S8.** Plot of  $\ln k_1'$  vs.  $\Sigma\sigma/2$  for the copolymerization reactions of 4-methylstyrene with CO (5 bar).

As it follows from what said above, the data corresponding to reactions that could be modeled by the approach described in the previous paragraph match the plot in Figure S3 quite closely and the same comments made previously apply here. The outcome of the reactions with the two most electron-withdrawing substituents also strengthen the ascending trend  $\ln k_1'$  vs.  $\Sigma\sigma/2$ . Given its low steric hindrance,  $[3,5-\text{F}_2\text{C}_6\text{H}_3]_2\text{-BIAN}$  may have been expected to give a more active catalyst than observed. However, for such a ligand that gives a low stability catalyst (see later), the assumption that catalyst decomposition is negligible at time zero may not be completely fulfilled and this may explain the slight anomaly. The ligand with 6 methoxy group is that which deviates more strongly from the value expected based on its  $\Sigma\sigma/2$  and steric hindrance. In general, ligands having an aryl group with three methoxy groups are those that fit less the correlation even for the reactions of unsubstituted styrene to be discussed in the following and  $[3,4,5-(\text{CH}_3\text{O})_3\text{C}_6\text{H}_2]_2\text{-BIAN}$  is that which deviates more from the correlation even with the latter substrate. It should be considered that the methoxy group has strong ad opposing inductive and resonance effects and the  $\Sigma\sigma$  value appears to afford a worse quantification of the electronic effects of the trimethoxyphenyl group than for other substituents. It should also be recalled that the catalytic reactions were run in trifluoroethanol, a solvent that gives strong hydrogen bonds. The methoxy oxygen is a likely donor for such hydrogen bonds and their formation would result in a decrease of the electron-donating properties of the trimethoxyphenyl group. As a matter of facts, the data for trimethoxy-substituted ligands statistically deviate from the general plot in the direction expected for a more electron-poor ligand.

As far as the catalyst decomposition rate is concerned, eq. 14 holds irrespective of the kinetics of the decomposition and may allow the calculation of a series of comparable decomposition rates at time zero, but the latter cannot be directly compared with the  $k_3$  values previously determined for some of the reactions. However, as long as the time zero data are concerned, it can be expected that deviation of the catalyst deactivation rate from that described in eq. 7 should be small, although such equation cannot be used to simulate the full data range in some cases. By combining eqs. 13 and 7 we get:

$$-\frac{d^2(\text{CO abs})}{dt^2} = -k_1 V \left( \frac{d[\text{Pd}^{\text{II}}]}{dt} \right) = -k_1 V (-k_3 [\text{Pd}^{\text{II}}]^2) \quad (17)$$

$$k_3 = \left( -\frac{d^2(\text{CO abs})}{dt^2} \right) / (k_1 V [\text{Pd}^{\text{II}}]^2) \quad (18)$$

Estimating again the constant values from the initial derivative and concentration data and taking into account eq. 16, we finally get:

$$k_3' = \left( -\frac{d^2(\text{CO abs})}{dt^2} \right)_0 / (k_1' V [\text{Pd}^{\text{II}}]_0^2) = -\left( \frac{d^2(\text{CO abs})}{dt^2} \right)_0 / \left( \frac{d(\text{CO abs})}{dt} \right)_0 [\text{Pd}^{\text{II}}]_0 \quad (19)$$

where the notation  $k_3'$  has been used analogously to what done before for  $k_1'$ .

It should be noted that the “catalyst decomposition rate” at time zero in eq. 14 and  $k_3'$  differ only by a constant factor,  $[\text{Pd}^{\text{II}}]^2$ . Thus exactly the same trends can be obtained by plotting either set of data. In order to allow at least a semiquantitative comparison between the data determined by the derivative approach and those derived from a fitting of the original data, we have chosen to work on  $k_3'$  values. The latter are included in Table S2 and a logarithmic plot is shown in Figure S9.

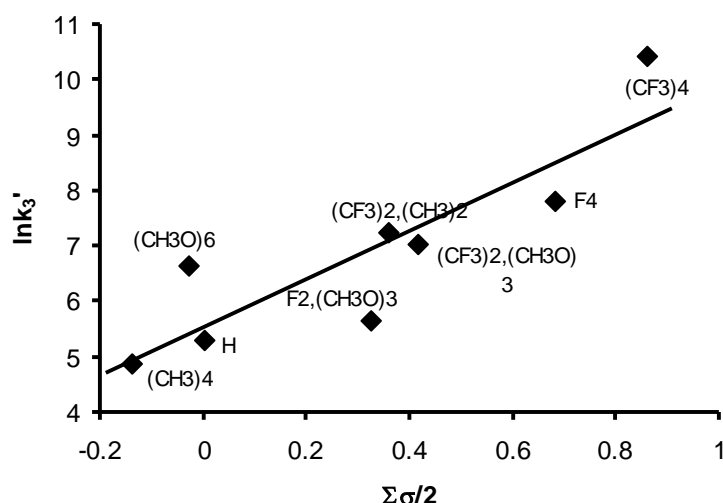


**Figure S9.** Plot of  $\ln k_3'$  vs.  $\Sigma\sigma/2$  for the copolymerization reactions of 4-methylstyrene with CO (5 bar).

The quantitative agreement between  $k_3'$  and  $k_3$  values is worse than in the case of  $k_1$ , but this was expected because now even the approximations involved in the determination of the second derivative are involved. In any case, the general pattern is not altered and the added data confirm the higher instability of the catalysts derived from electron-poor ligands. Again the methoxy-substituted ligands are those that statistically deviate more from the correlation.

### **Fitting of the data of the styrene experiments run under 5 bar CO**

A series of experiments paralleling those just described, but employing unsubstituted styrene as substrate was also performed. The resulting CO absorption plots are shown in Figure S10. The experiment using 3,5-(CF<sub>3</sub>)<sub>2</sub>C<sub>6</sub>H<sub>3</sub>;3,4,5-(CH<sub>3</sub>O)<sub>3</sub>C<sub>6</sub>H<sub>2</sub>-BIAN as ligand gave some problems and has been discarded.

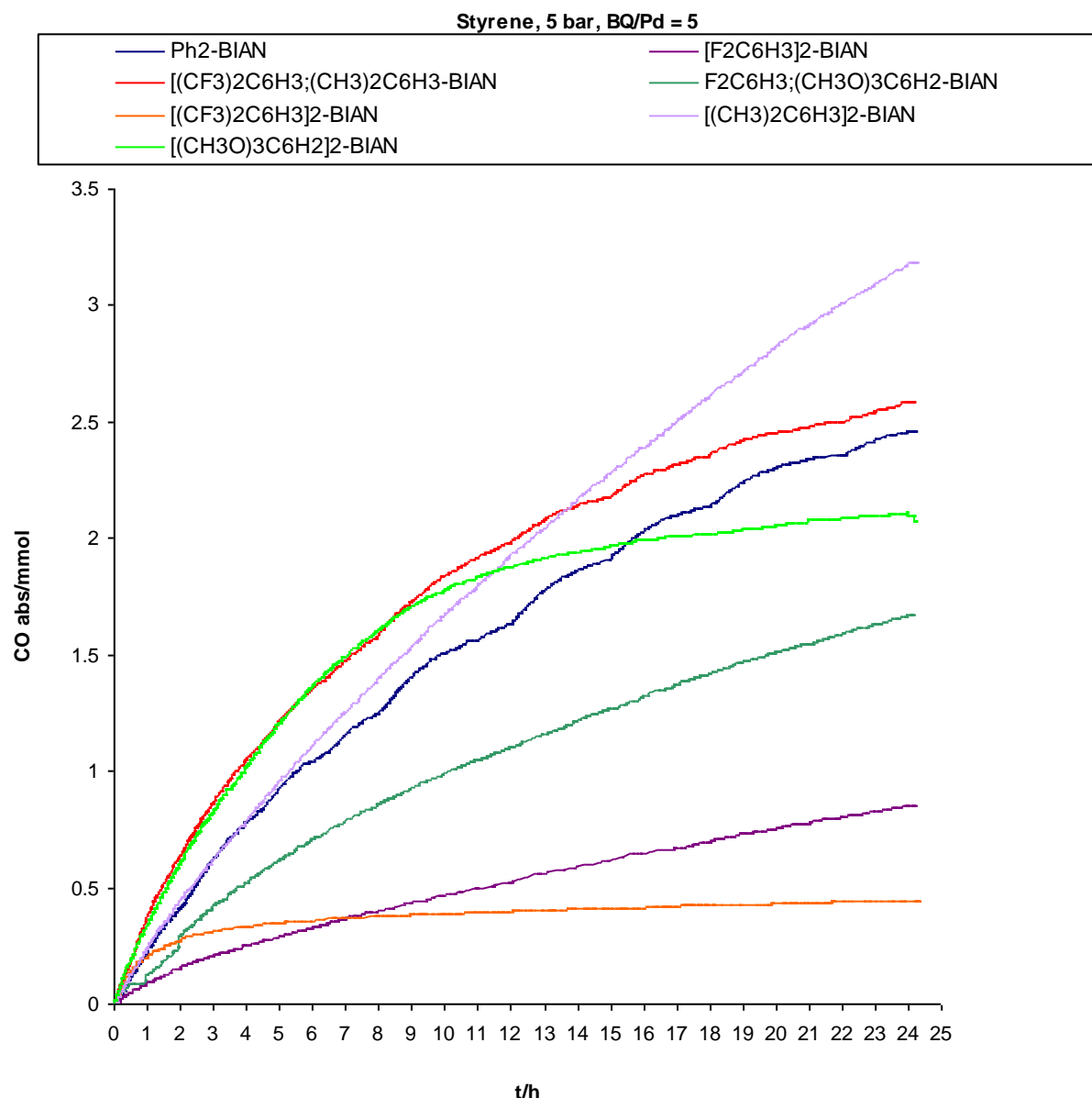


**Figure S10.** CO absorption plot for the copolymerization of methylstyrene under 5 bar CO ( $[BQ]/[Pd] = 5$ ) catalyzed by different  $[Pd(CH_3)(CH_3CN)(Ar-BIAN)][PF_6]$  complexes as catalysts.

The data were subjected to the same mathematical treatment described for those of the 4-methylstyrene reactions. Given the negative results previously obtained with the first order decomposition model, only the fit to the second order one was performed. The same three ligands that had failed to give data series that could be fitted by eq. 10 in the case of 4-methylstyrene also gave a poor fit in the present case, which leaves only four data points for which very good results were obtained. The calculated values of  $k_1$  and  $k_3$  are reported in Table S3 and graphically represented in figures S11 and S12.

**Table S3.** Fitting of four reactions run with styrene under 5 bar CO ( $[BQ]/[Pd] = 5$ ) by equation 10.

Ligand	$\Sigma\sigma/2$	$k_1/h^{-1}$	$k_3/h^{-1}M^{-1}$
$[3,5-(CH_3)_2C_6H_3]_2$	-0.14	208	494
Ph <sub>2</sub> -BIAN	0	231	1126
3,5-F <sub>2</sub> C <sub>6</sub> H <sub>3</sub> ;3,4,5-(CH <sub>3</sub> O) <sub>3</sub> C <sub>6</sub> H <sub>2</sub> -BIAN	0.325	153	1112
3,5-(CH <sub>3</sub> ) <sub>2</sub> C <sub>6</sub> H <sub>3</sub> ;3,5-(CF <sub>3</sub> ) <sub>2</sub> C <sub>6</sub> H <sub>3</sub> -BIAN	0.36	425	3045

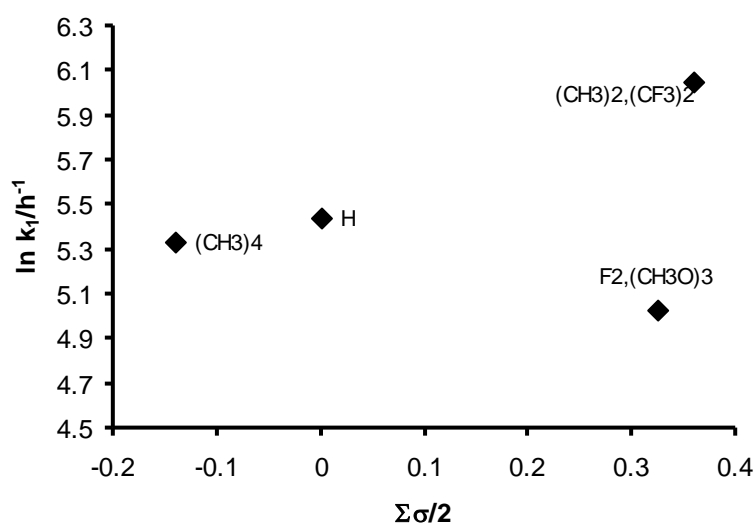


**Figure S11.** Logarithmic plot of  $k_1$  with respect to  $\Sigma\sigma/2$ . Data from Table S3.

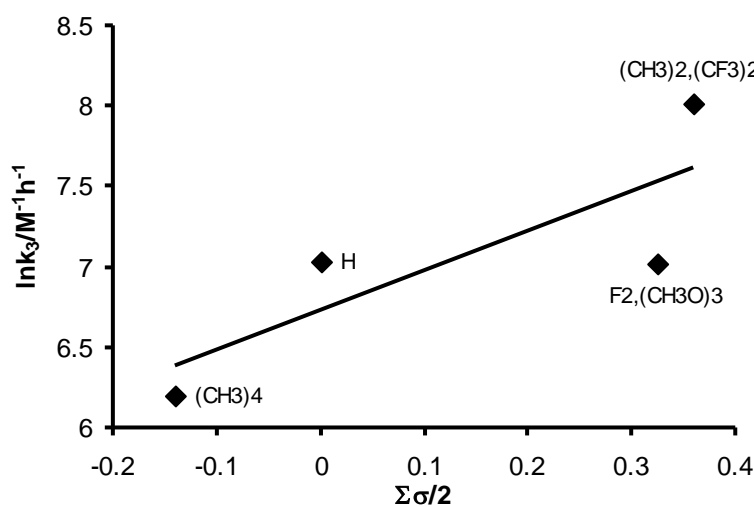


**Figure S12.** Logarithmic plot of  $k_3$  with respect to  $\Sigma\sigma/2$ . Data from Table S3.

With the exception of the  $k_1$  value for  $3,5\text{-F}_2\text{C}_6\text{H}_3;3,4,5\text{-(CH}_3\text{O})_3\text{C}_6\text{H}_2\text{-BIAN}$ , the data follow the same trend evidenced for the 4-methylstyrene experiments, that is electron-withdrawing substituents lead to more active, but less stable, catalytic systems.

To get information even from the remaining three reactions, the same interpolation/differentiation procedure described for 4-methylstyrene was then applied. The first and second derivative plots are shown in figures S13 and S14 respectively.

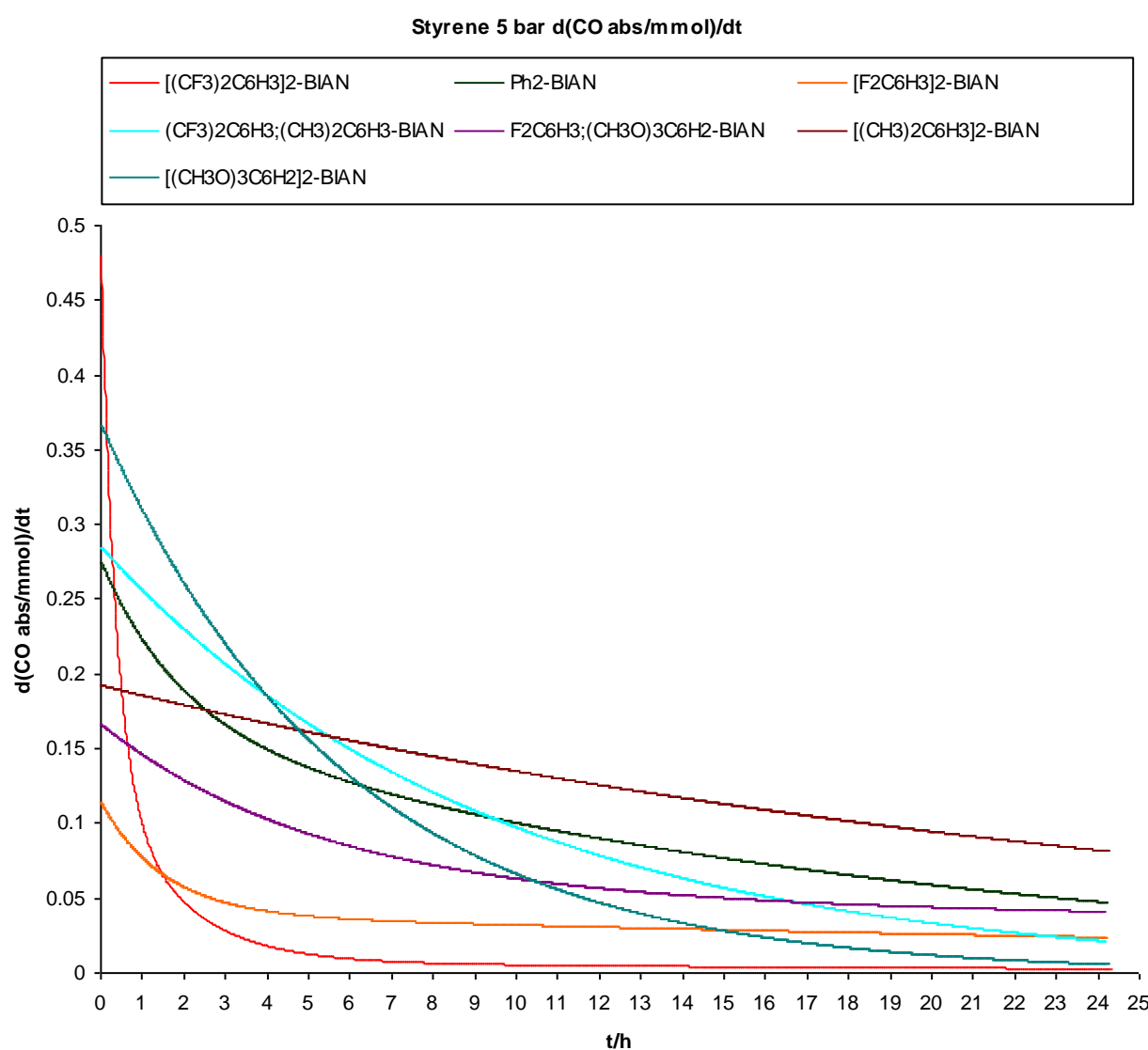


**Figure S13.**

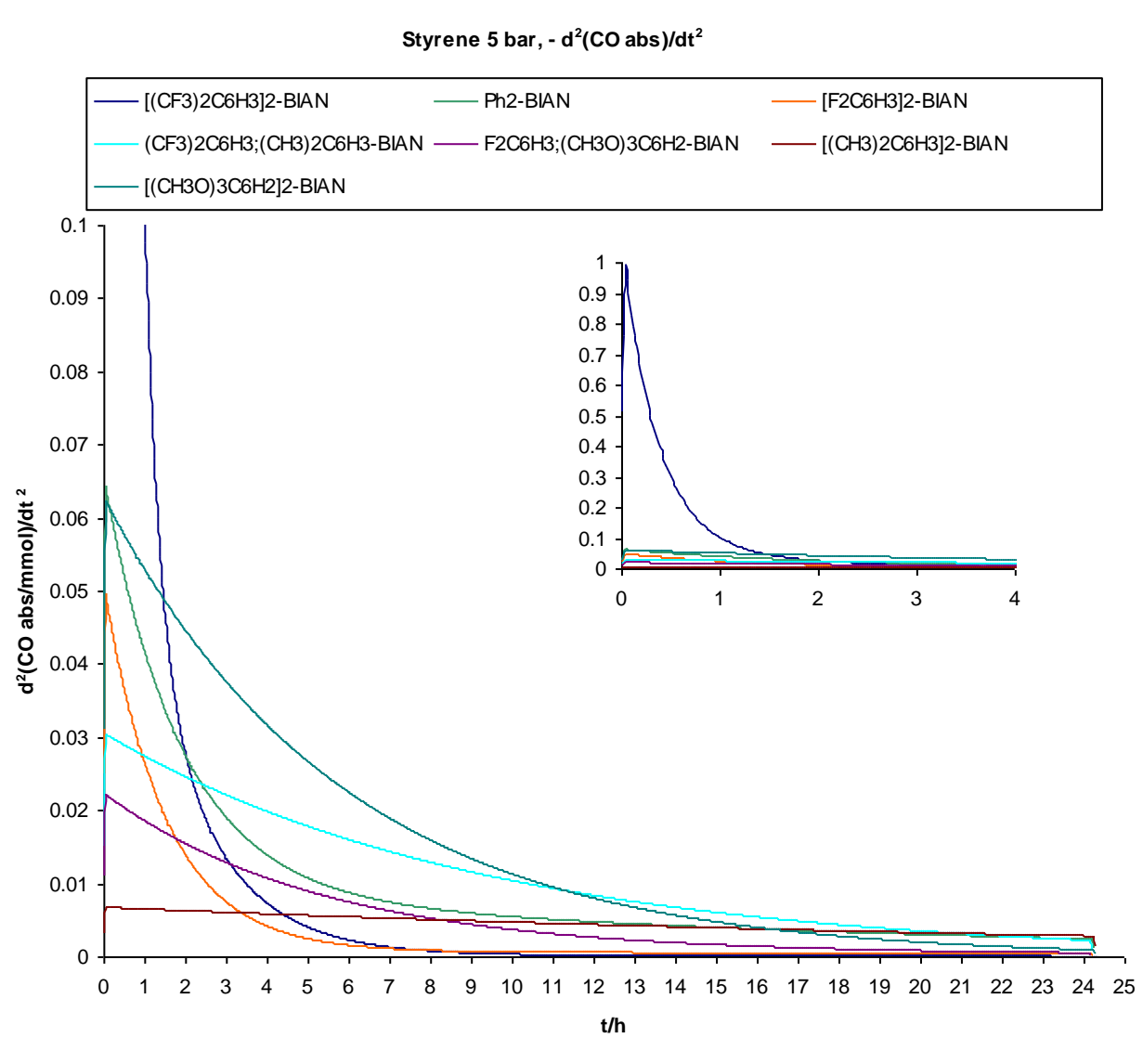


**Figure S14.** The inset shows the full scale plot for the first four hours.

From these plots, the value of  $k_1'$  and  $k_3'$  can be calculated as described for the 4-methylstyrene reactions. Results are reported in Table S4 and logarithmic plots of  $k_1'$  and  $k_3'$  vs.  $\Sigma\sigma/2$  are shown in figures S15 and S16 respectively.

**Table S4:** Values of  $k_1'$  and  $k_3'$  calculated from eqs. 16 and 19 for of all reactions run with styrene under 5 bar CO ( $[BQ]/[Pd] = 5$ ).

Ligand	$\Sigma\sigma/2$	$k_1'/h^{-1}$	$k_3'/h^{-1}M^{-1}$
[3,5-(CH <sub>3</sub> ) <sub>2</sub> C <sub>6</sub> H <sub>3</sub> ] <sub>2</sub> -BIAN	-0.14	234	2.08×10 <sup>2</sup>
[3,4,5-(CH <sub>3</sub> O) <sub>3</sub> C <sub>6</sub> H <sub>2</sub> ] <sub>2</sub> -BIAN	-0.03	503	8.88×10 <sup>2</sup>
Ph <sub>2</sub> -BIAN	0	213	2.16×10 <sup>3</sup>
3,5-F <sub>2</sub> C <sub>6</sub> H <sub>3</sub> ;3,4,5-(CH <sub>3</sub> O) <sub>3</sub> C <sub>6</sub> H <sub>2</sub> -BIAN	0.325	157	4.60×10 <sup>2</sup>
3,5-(CH <sub>3</sub> ) <sub>2</sub> C <sub>6</sub> H <sub>3</sub> ;3,5-(CF <sub>3</sub> ) <sub>2</sub> C <sub>6</sub> H <sub>3</sub> -BIAN	0.36	358	6.09×10 <sup>2</sup>
[3,5-F <sub>2</sub> C <sub>6</sub> H <sub>3</sub> ] <sub>2</sub> -BIAN	0.68	85	4.17×10 <sup>3</sup>
[3,5-(CF <sub>3</sub> ) <sub>2</sub> C <sub>6</sub> H <sub>3</sub> ] <sub>2</sub> -BIAN	0.86	422	1.67×10 <sup>4</sup>

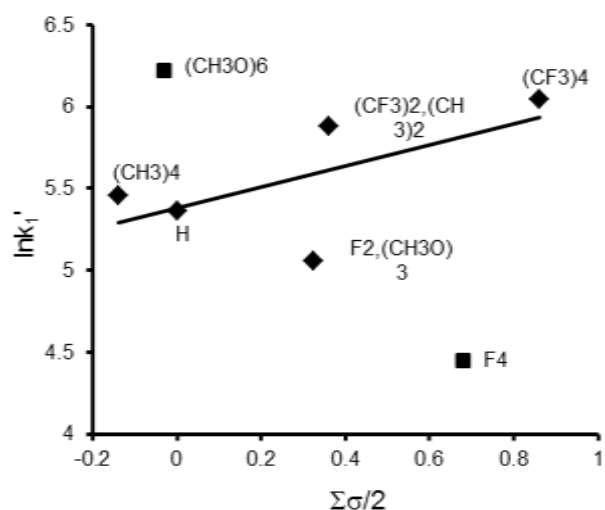


**Figure S15.** Plot of  $\ln k_1'$  vs.  $\Sigma\sigma/2$  for the copolymerization reactions of styrene with CO (5 bar). The straight line corresponds to the best fit to the data points, excluding those for [3,4,5-(CH<sub>3</sub>O)<sub>3</sub>C<sub>6</sub>H<sub>2</sub>]<sub>2</sub>-BIAN and [3,5-F<sub>2</sub>C<sub>6</sub>H<sub>3</sub>]<sub>2</sub>-BIAN.

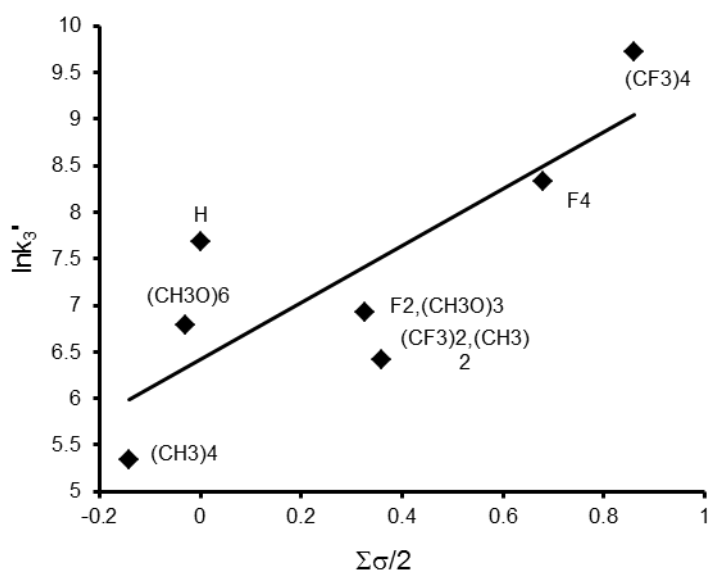


**Figure S16.** Plot of  $\ln k_3'$  vs.  $\Sigma\sigma/2$  for the copolymerization reactions of styrene with CO (5 bar) The straight line corresponds to the best fit to all data points.

As in the case of 4-methylstyrene, there is a good agreement between corresponding  $k_1$  and  $k_1'$  values and a worse agreement between  $k_3$  and  $k_3'$  values, but the general trends are maintained. The  $k_1'$  value for  $[3,5\text{-F}_2\text{C}_6\text{H}_3]_2\text{-BIAN}$  appears to be abnormally low. Given the general shape of the first and second derivative plots for this ligand, the best explanation for this anomalous value is that catalyst deactivation has proceeded to a relatively large extent in the pre-time zero period, resulting in an underestimation of the time zero values for both derivatives. The effect is not observable on the  $k_3'$  value since this value derives from a quotient of the two derivatives values and underestimation of both results in a compensation of the errors.

In general the data follow the same trend evidenced for the 4-Me-styrene experiments, that is electron-withdrawing substituents lead to more active, but less stable, catalytic systems.

Overall, the data also confirm the general tendency that reactions with styrene are faster than those with 4-methylstyrene, but the catalyst decomposes more quickly. The faster deactivation is responsible for the less good agreement between  $k_1$  and  $k_1'$  and  $k_3$  and  $k_3'$  values, since all approximations become larger.

A more interesting comparison can be made between the corresponding  $k_1$  (or  $k_1'$ ) and  $k_3$  (or  $k_3'$ ) values for the two substrates. In a previous paper in which some of the same ligands here employed had been tested, it had been noted that a higher productivity was obtained with unsubstituted styrene,<sup>10</sup> contrary to what generally reported in the literature.<sup>11,12-15</sup> The new, more extensive, series of data supports this observation, but also shows that the higher activity is also associated

with a faster deactivation, since not only  $k_1$ , but also  $k_3$  values are consistently higher in the case of styrene. To the best of our knowledge, an active role of the olefin in the deactivation process has not been proposed before. We will discuss this aspect in more detail later, after having reported the rest of the results.

The faster deactivation is responsible for the less good agreement between  $k_1$  and  $k_1'$  and  $k_3$  and  $k_3'$  values, since all approximations become larger.

### Effect of CO pressure

To investigate the effect of the carbon monoxide pressure, a few reactions were performed under either 3 or 10 bar CO. The outcome of these reactions is compared with that of the 5 bar reactions with the corresponding ligands in figures S17 and S18.

**F2C6H3;(CH3O)3C6H3-BIAN, styrene,  
BQ=5, 3, 5, 10 bar**

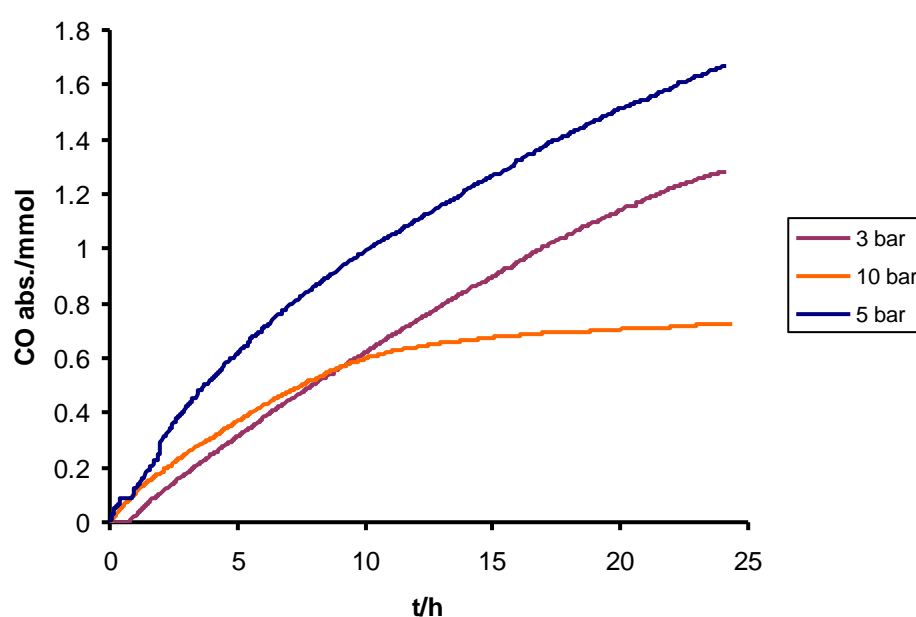


**Figure S17.**

**(CH<sub>3</sub>)<sub>2</sub>C<sub>6</sub>H<sub>3</sub>;(CF<sub>3</sub>)<sub>2</sub>C<sub>6</sub>H<sub>3</sub>-BIAN, styrene 3, 5 bar**

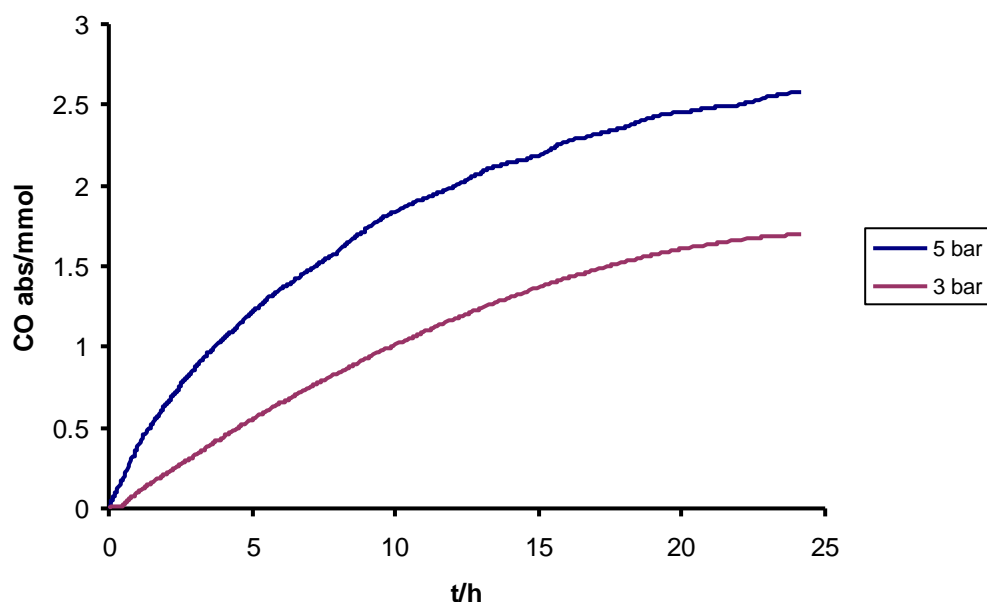


**Figure S18.**

We first attempted fitting the data by eq. 10. We have previously mentioned that reactions run under 3 bar gave an anomalous behavior (a flat section) in the CO absorption plot and we discussed the physical reasons for that. To fit the data without being affected by this instrumental artifact, the meaningless data were ignored and eq. 10 was modified by the addition of a further “offset” parameter (c in eq. 20) that allows modeling of a curve that does not pass through the axes origin.

$$(\text{CO abs})/V = (k_1/k_3)\ln(1+k_3[\text{Pd}^{\text{II}}]_0t) + c \quad (20)$$

The fitted values are reported in Tables S5 and S6, together with the corresponding  $k_1'$  and  $k_3'$  values, calculated as in the other cases. Note that the values for the reactions at 5 bar are the same previously included in Table S3 and are shown again here for an immediate comparison.

**Table S5.**  $k_1$  and  $k_1'$  values for reactions run at different CO pressures with different ligands (styrene as substrate,  $[BQ]/[Pd] = 5$ )

Ligand		3 bar	5 bar	10 bar
3,5-F <sub>2</sub> C <sub>6</sub> H <sub>3</sub> ;3,4,5-(CH <sub>3</sub> O) <sub>3</sub> C <sub>6</sub> H <sub>2</sub> -BIAN	$k_1$	77	153	
	$k_1'$	73	157	125
3,5-(CH <sub>3</sub> ) <sub>2</sub> C <sub>6</sub> H <sub>3</sub> ;3,5-(CF <sub>3</sub> ) <sub>2</sub> C <sub>6</sub> H <sub>3</sub> -BIAN	$k_1$	124	425	
	$k_1'$	125	358	

**Table S6.**  $k_3$  and  $k_3'$  values for reactions run at different CO pressures with different ligands (styrene as substrate,  $[BQ]/[Pd] = 5$ )

Ligand		3 bar	5 bar	10 bar
3,5-F <sub>2</sub> C <sub>6</sub> H <sub>3</sub> ;3,4,5-(CH <sub>3</sub> O) <sub>3</sub> C <sub>6</sub> H <sub>2</sub> -BIAN	$k_3$	$3.12 \times 10^2$	$1.11 \times 10^3$	
	$k_3'$	$2.16 \times 10^2$	$1.01 \times 10^3$	$1.03 \times 10^3$
3,5-(CH <sub>3</sub> ) <sub>2</sub> C <sub>6</sub> H <sub>3</sub> ;3,5-(CF <sub>3</sub> ) <sub>2</sub> C <sub>6</sub> H <sub>3</sub> -BIAN	$k_3$	$1.07 \times 10^3$	$3.05 \times 10^3$	
	$k_3'$	$3.66 \times 10^2$	$6.09 \times 10^2$	

The reactions under 5 bar are faster than those under 3 bar, but a further increase in pressure leads to a decrease in activity.<sup>16</sup> The additional information we get from the numerical simulations is that the decrease in productivity on going to 10 bar is not due to a faster catalyst deactivation in the last case. Indeed even  $k_1$  or  $k_1'$  decrease at 10 bar and moreover the values of  $k_3$  and  $k_3'$  increases on going from 3 to 5 bar, but are of the same order of magnitude for reactions run at 5 or 10 bar. This indicates that rate of deactivation is higher under 5 rather than 3 bar CO, but no faster deactivation takes place at higher CO pressures. Thus the decrease in activity in the latter case is due to the inhibiting role of CO. This is a phenomenon well known for this reaction and the value of CO pressure at which this effect becomes evident depends on the catalyst nature, if dicationic or monocationic precatalysts are applied, and on the nature of the ancillary ligand bonded to palladium.

In addition, the rate ( $k_1$  or  $k_1'$ ) increase on going from 3 to 5 bar is higher than the 5/3 ratio that would be expected for a first order kinetics with respect to CO pressure. This indicates a complex dependence of the reaction rate on CO pressure, but the data collected in this work are insufficient to discuss this aspect in any detail.

### Effect of a longer reaction time and a larger amount of benzoquinone

The effect of a longer reaction time was investigated by running a series of reactions under 10 bar CO for 70 h instead of 25. Since it was expected that deactivation would occur, a higher benzoquinone amount (mol ratio BQ/Pd = 40) was also added. Results are graphically shown in Figure S19.

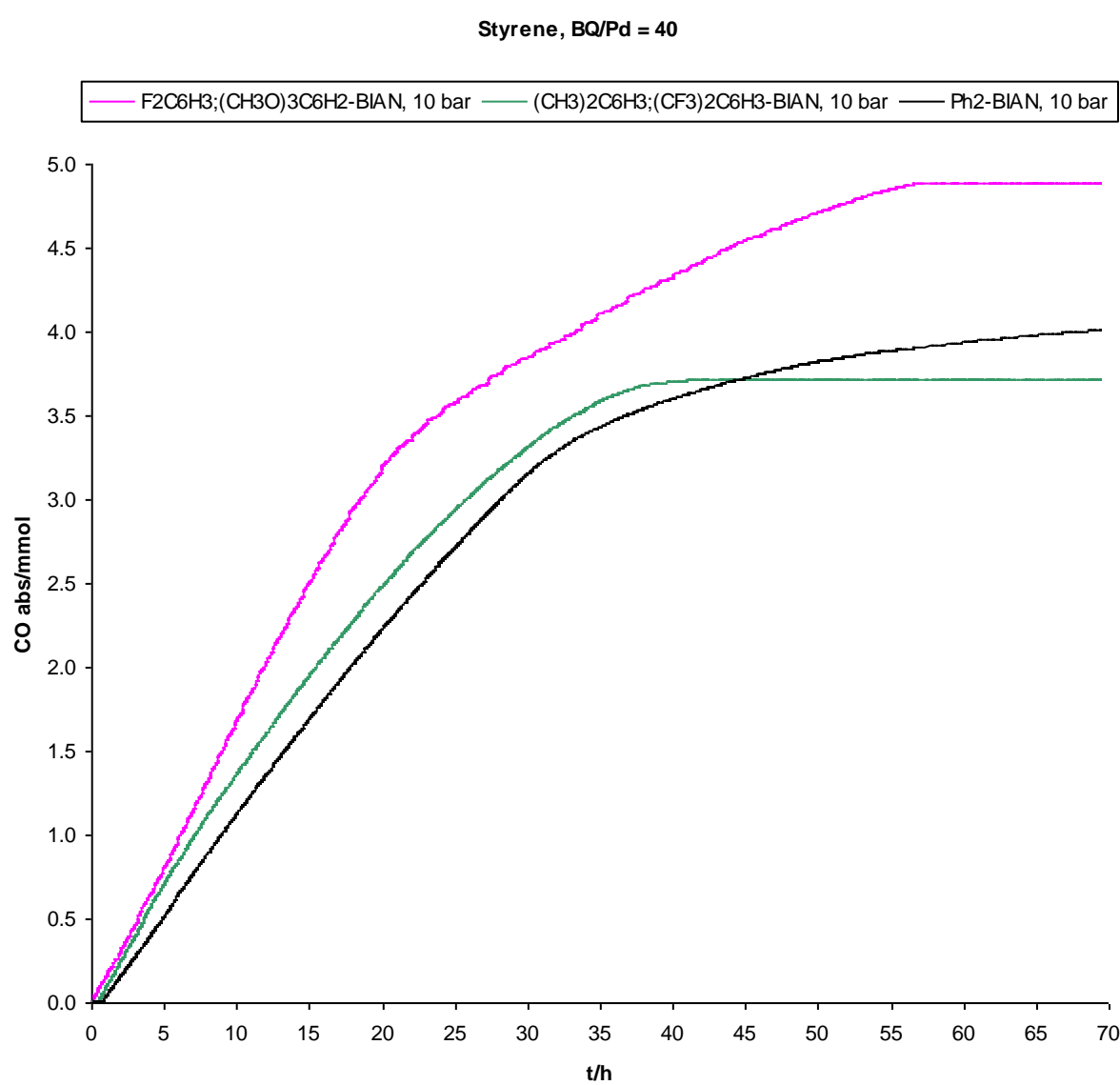


**Figure S19.** Reactions run for a longer time and with  $[BQ]/[Pd] = 40$ .

From Figure S19 it is evident that the addition of a larger amount of benzoquinone strongly stabilizes the catalytic system. Deactivation is very low during the first 24 hours, contrary to what previously observed under the same conditions, but with  $[BQ]/[Pd] = 5$ . The rate decrease that is observed in all cases after about 3.2 mmol CO have been absorbed is at least partly due to the

precipitation of the growing polymer chain with the switch of the catalytic system from homogeneous to a mixture of homogeneous and heterogeneous species, each of them displaying its own kinetic behavior. Thus this decrease cannot be described by our models and we have limited the modeling to the first 24 h of reaction. Due to the increased catalyst stability, good fitting by the second order deactivation mode was obtained in all cases, but in order to have a direct comparison with data with the lower benzoquinone amount,  $k_1'$  and  $k_3'$  values were also calculated. All constant values are reported in Table S7. A good agreement exists between the two calculation approaches, except for the  $k_3'$  value for 3,5-(CH<sub>3</sub>)<sub>2</sub>C<sub>6</sub>H<sub>3</sub>;3,5-(CF<sub>3</sub>)<sub>2</sub>C<sub>6</sub>H<sub>3</sub>-BIAN, which appears to be overestimated.

**Table S7:** Values of  $k_1$ ,  $k_3$ ,  $k_1'$  and  $k_3'$  for reactions run with styrene, under 10 bar CO and with  $[BQ]/[Pd] = 40$ .

Ligand	$\Sigma\sigma/2$	$k_1/h^{-1}$	$k_3/h^{-1}M^{-1}$	$k_1'/h^{-1}$	$k_3'/h^{-1}M^{-1}$
Ph <sub>2</sub> -BIAN	0	125	107	124	92
3,5-F <sub>2</sub> C <sub>6</sub> H <sub>3</sub> ;3,4,5-(CH <sub>3</sub> O) <sub>3</sub> C <sub>6</sub> H <sub>2</sub> -BIAN	0.325	177	157	188	170
3,5-(CH <sub>3</sub> ) <sub>2</sub> C <sub>6</sub> H <sub>3</sub> ;3,5-(CF <sub>3</sub> ) <sub>2</sub> C <sub>6</sub> H <sub>3</sub> -BIAN	0.36	159	265	167	438

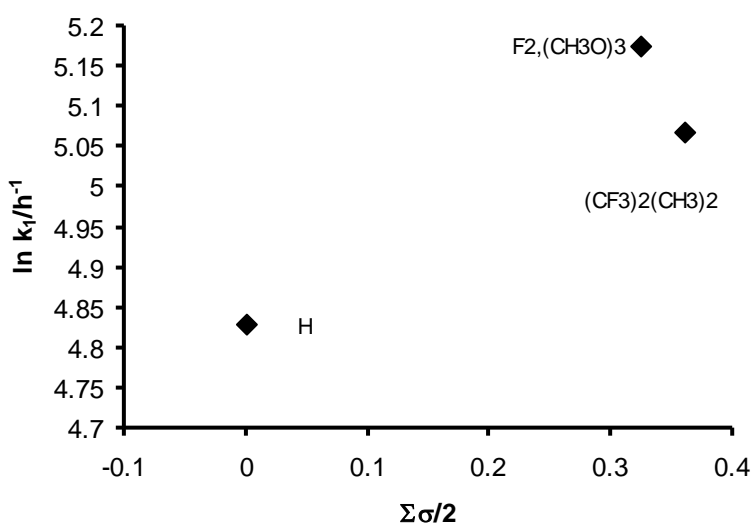


**Figure S20.** Reactions run for a longer time and with  $[BQ]/[Pd] = 40$ .

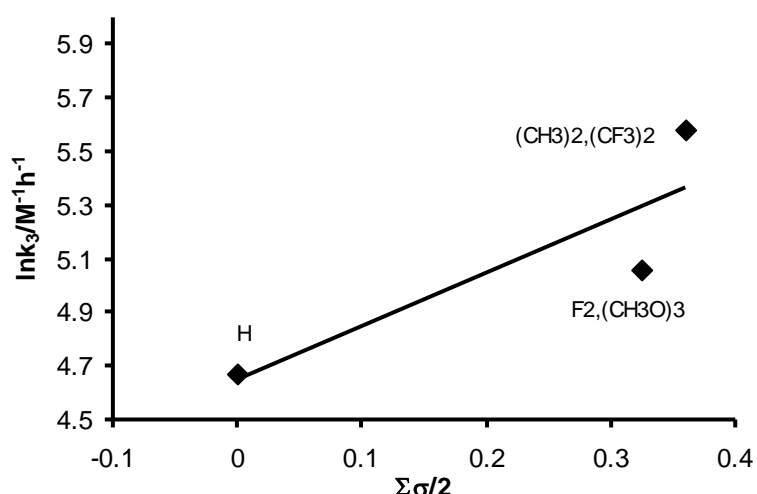


**Figure S21.** Reactions run for a longer time and with  $[\text{BQ}]/[\text{Pd}] = 40$ .

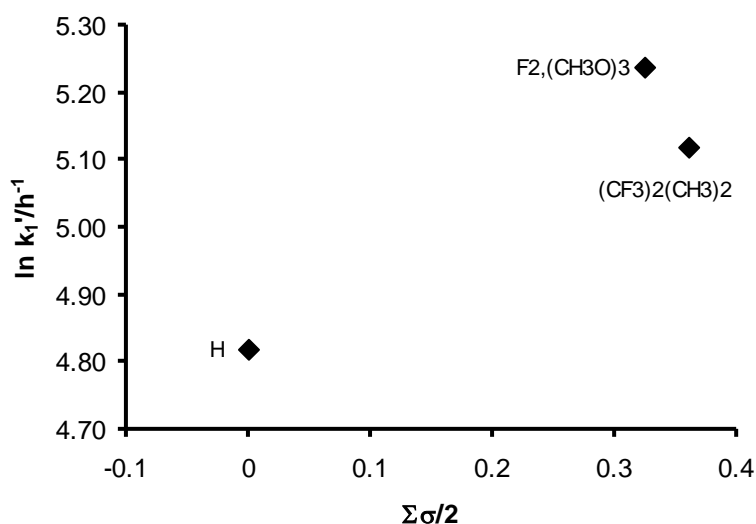


**Figure S22.** Reactions run for a longer time and with  $[\text{BQ}]/[\text{Pd}] = 40$ .

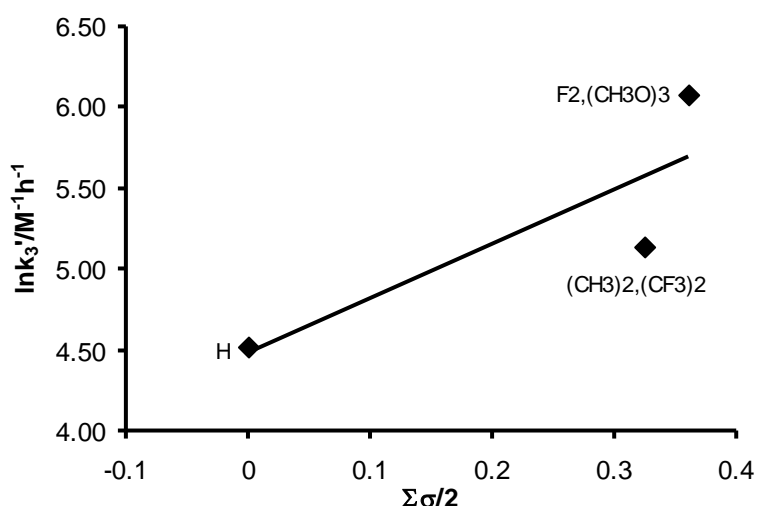


**Figure S23.** Reactions run for a longer time and with  $[BQ]/[Pd] = 40$ .

Only one direct comparison can be made with reactions run under exactly the same conditions, but with a ratio  $[BQ]/[Pd] = 5$ , that involving  $3,5-F_2C_6H_3;3,4,5-(CH_3O)_3C_6H_2$ -BIAN. The  $k_1'$  value marginally increased (from 125 to 188) upon an increase in benzoquinone amount, which may be due to the aforementioned approximations in neglecting the deactivation before the gas consumption starts to be measured. However, it is  $k_3'$  that is most affected, decreasing from  $1.03 \times 10^3$  to 170. This is in accord with a role of benzoquinone affecting catalyst stability and not catalytic rate.

For a discussion of further details of the catalyst decomposition pathway see the corresponding paragraph in paper text.

**Figure S24.**  $^1\text{H}$  NMR spectrum of ligand **3** ( $\text{CDCl}_3$ , 400 MHz, 298K).

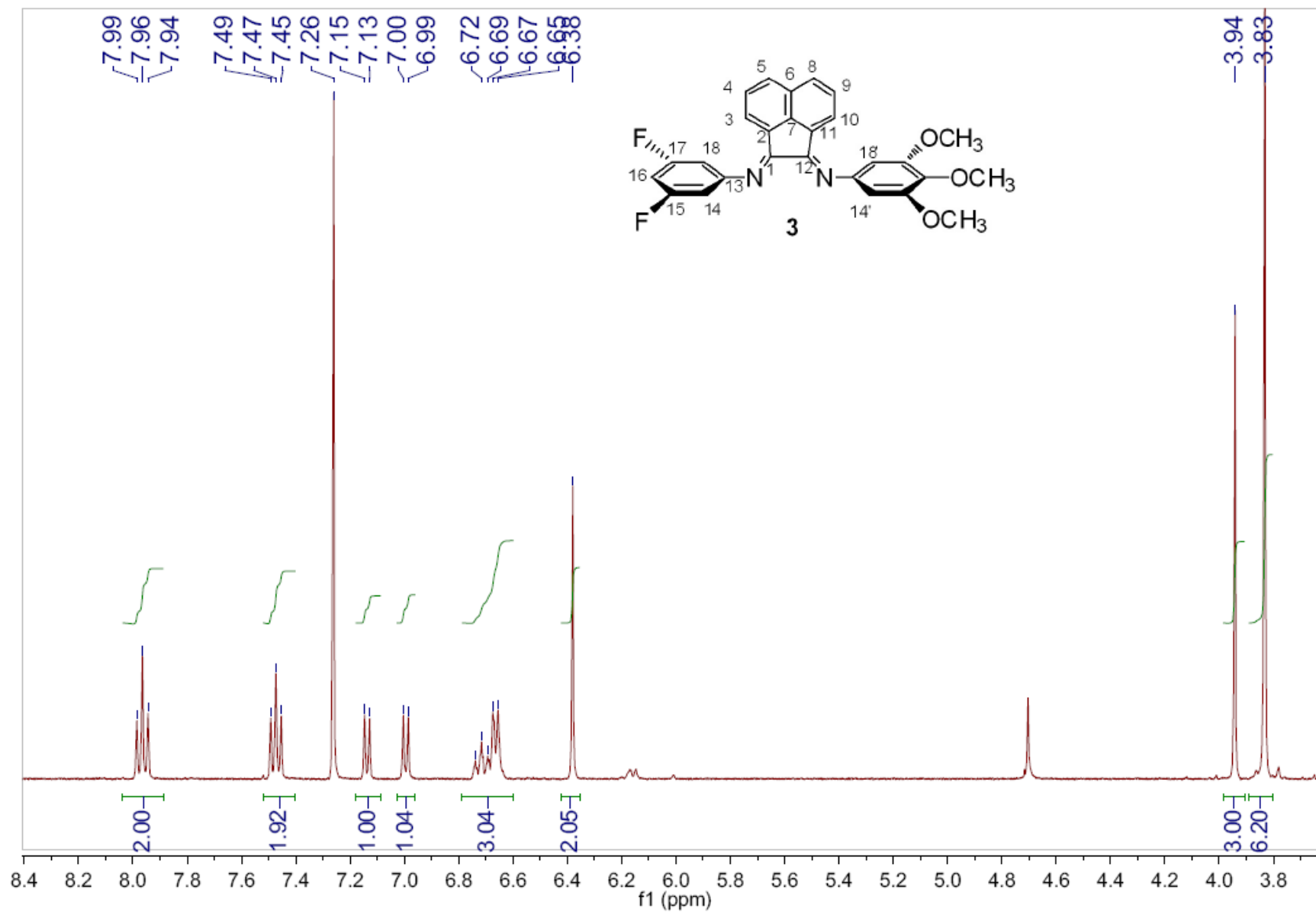


**Figure S25.**  $^{13}\text{C}$  NMR spectrum of ligand **3** (75MHz,  $\text{CDCl}_3$ , 298 K).

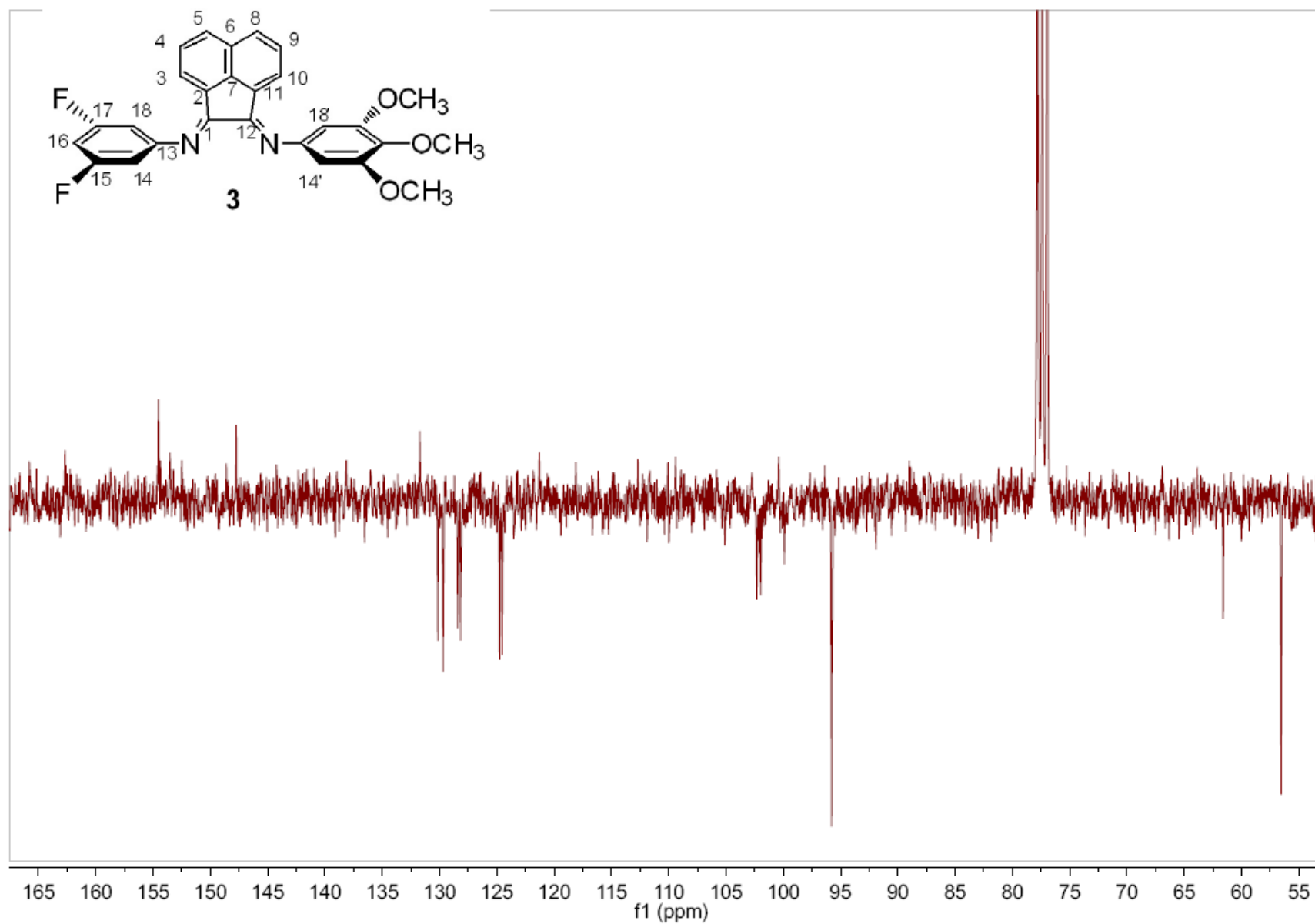


**Figure S26.**  $^{19}\text{F}\{^1\text{H}\}$  NMR spectrum of ligand **3** (376 MHz,  $\text{CDCl}_3$ , 298 K).

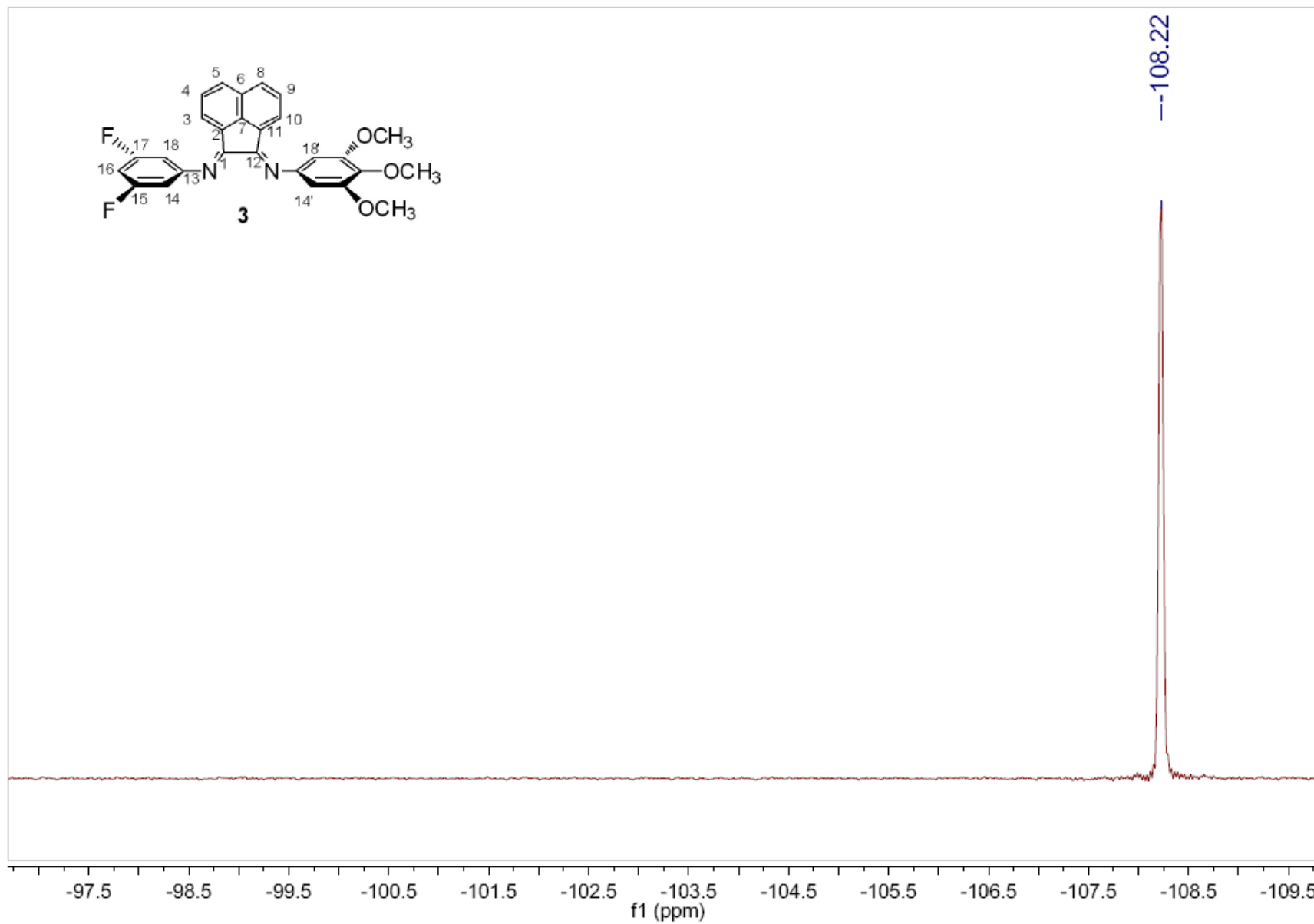


**Figure S27.**  $^1\text{H}$  NMR spectrum of ligand **7** ( $\text{CDCl}_3$ , 400 MHz, 298K).

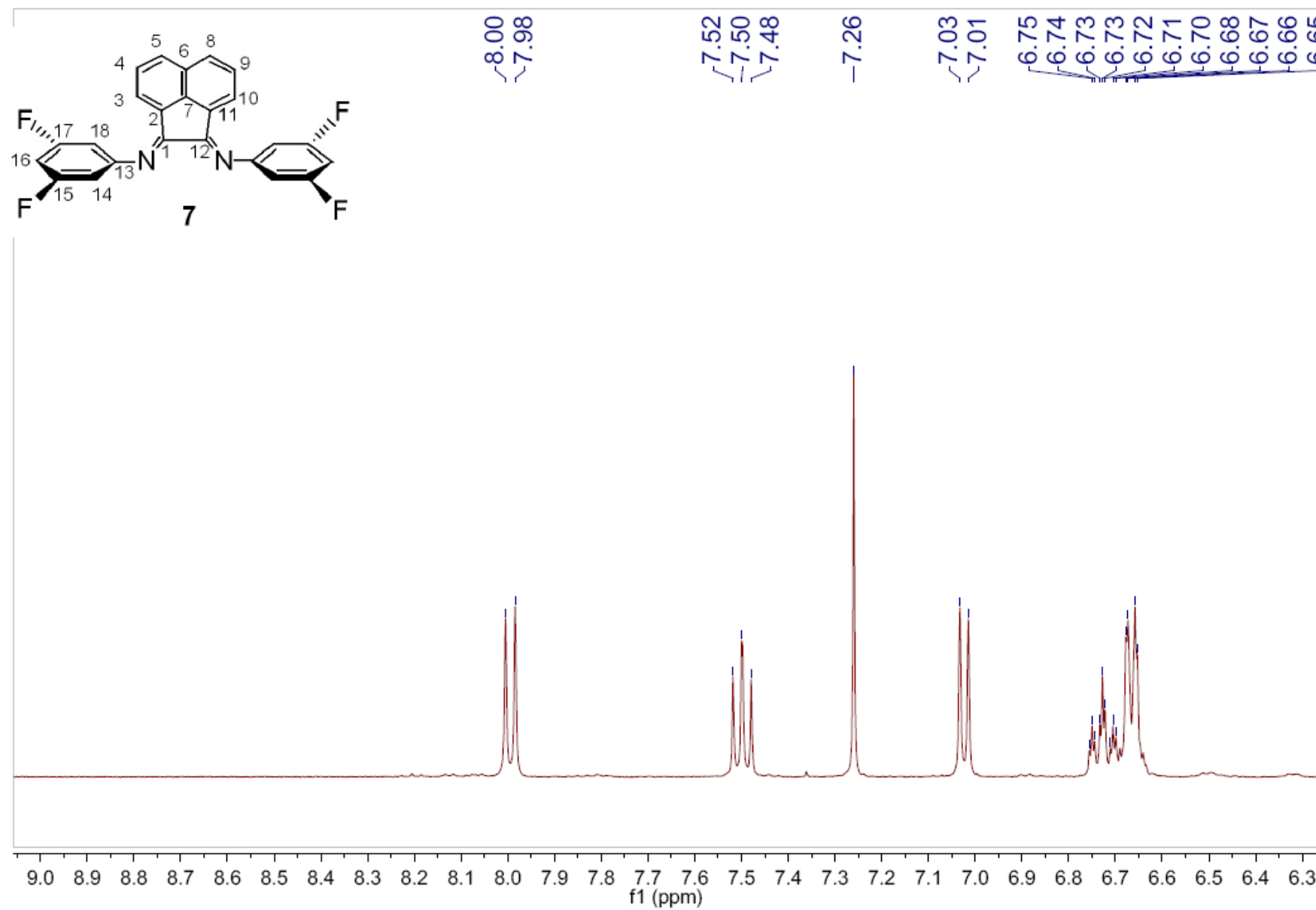


**Figure S28.**  $^{13}\text{C}$  NMR spectrum of ligand **7** (75MHz,  $\text{CDCl}_3$ , 298 K).

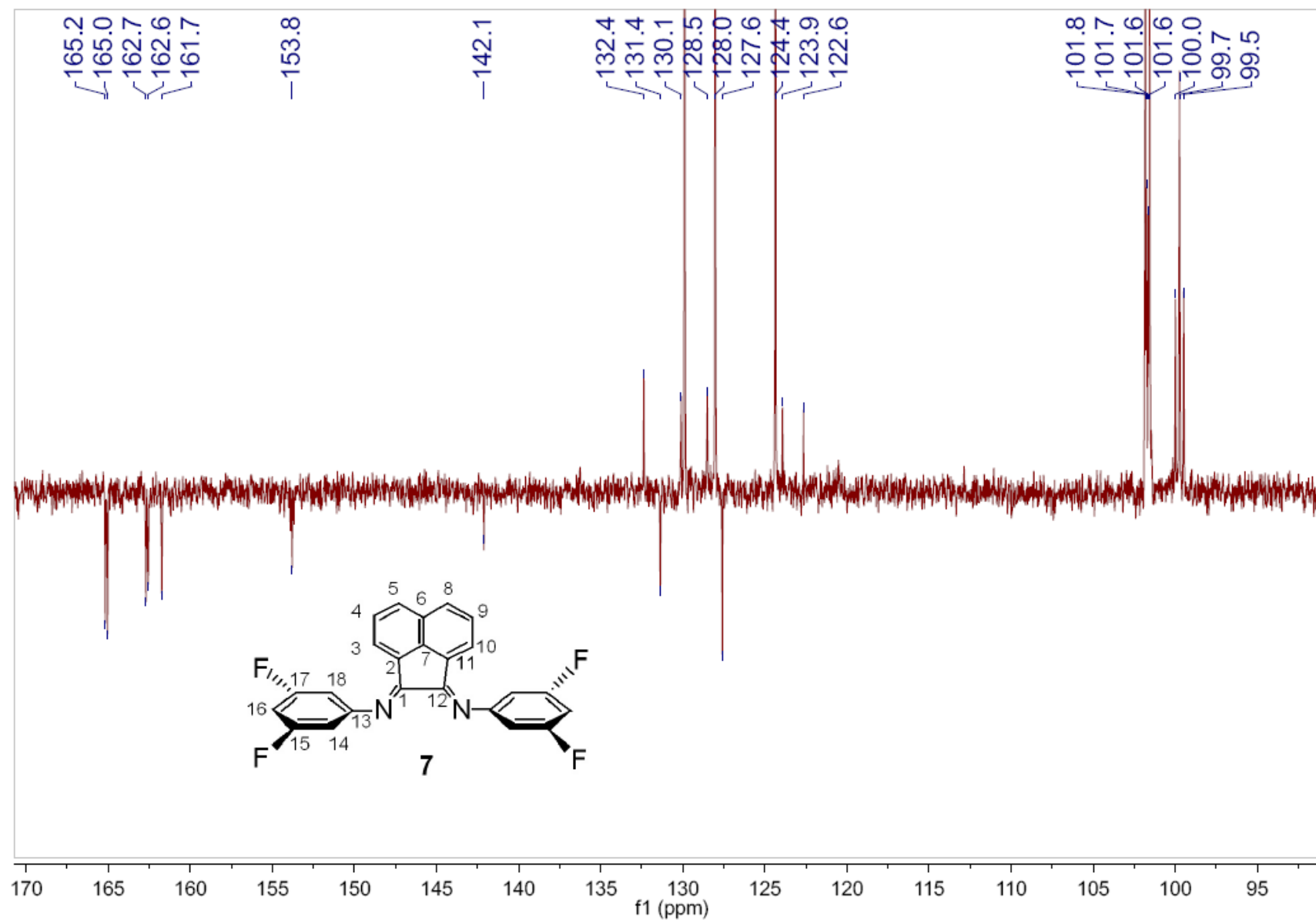
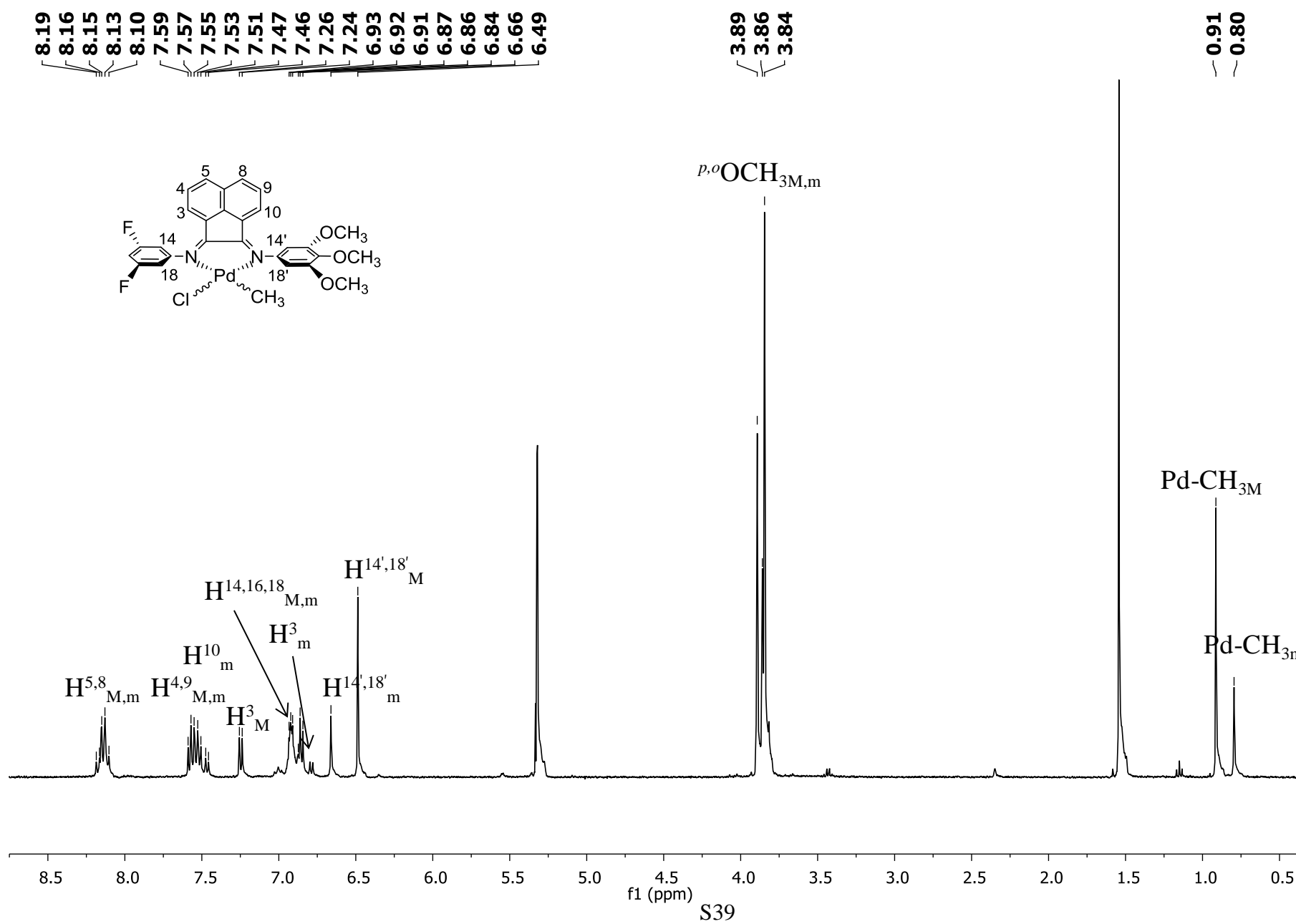
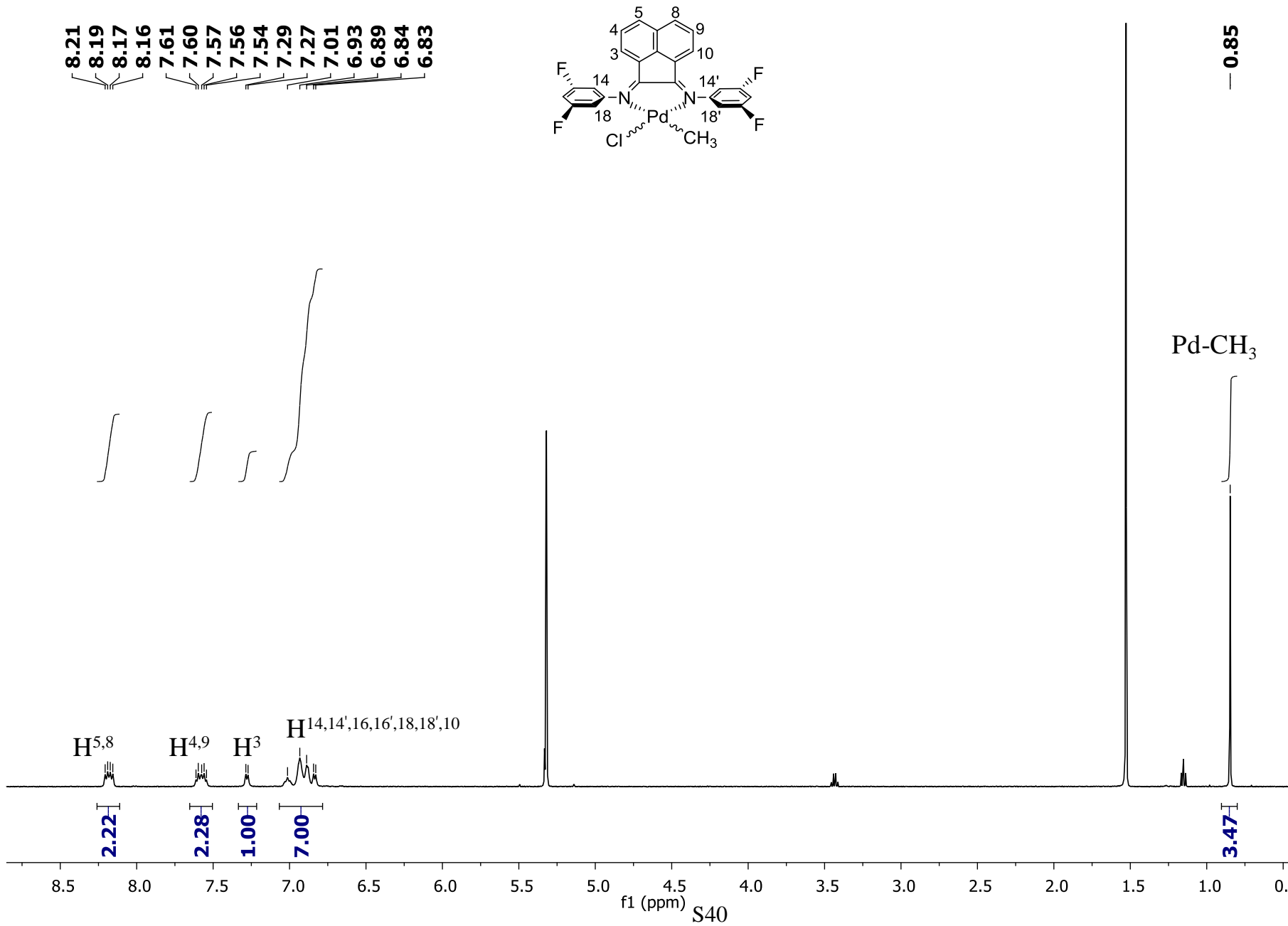


Figure S29.  $^1\text{H}$  NMR spectrum of complex **3a** ( $\text{CD}_2\text{Cl}_2$ , 500 MHz, 298 K).



**Figure S30.**  $^1\text{H}$  NMR spectrum of complex **7a** ( $\text{CD}_2\text{Cl}_2$ , 500 MHz, 298 K).



**Figure S31.**  $^1\text{H}$  NMR spectrum of complex **3b** ( $\text{CD}_2\text{Cl}_2$ , 500 MHz, 298 K)

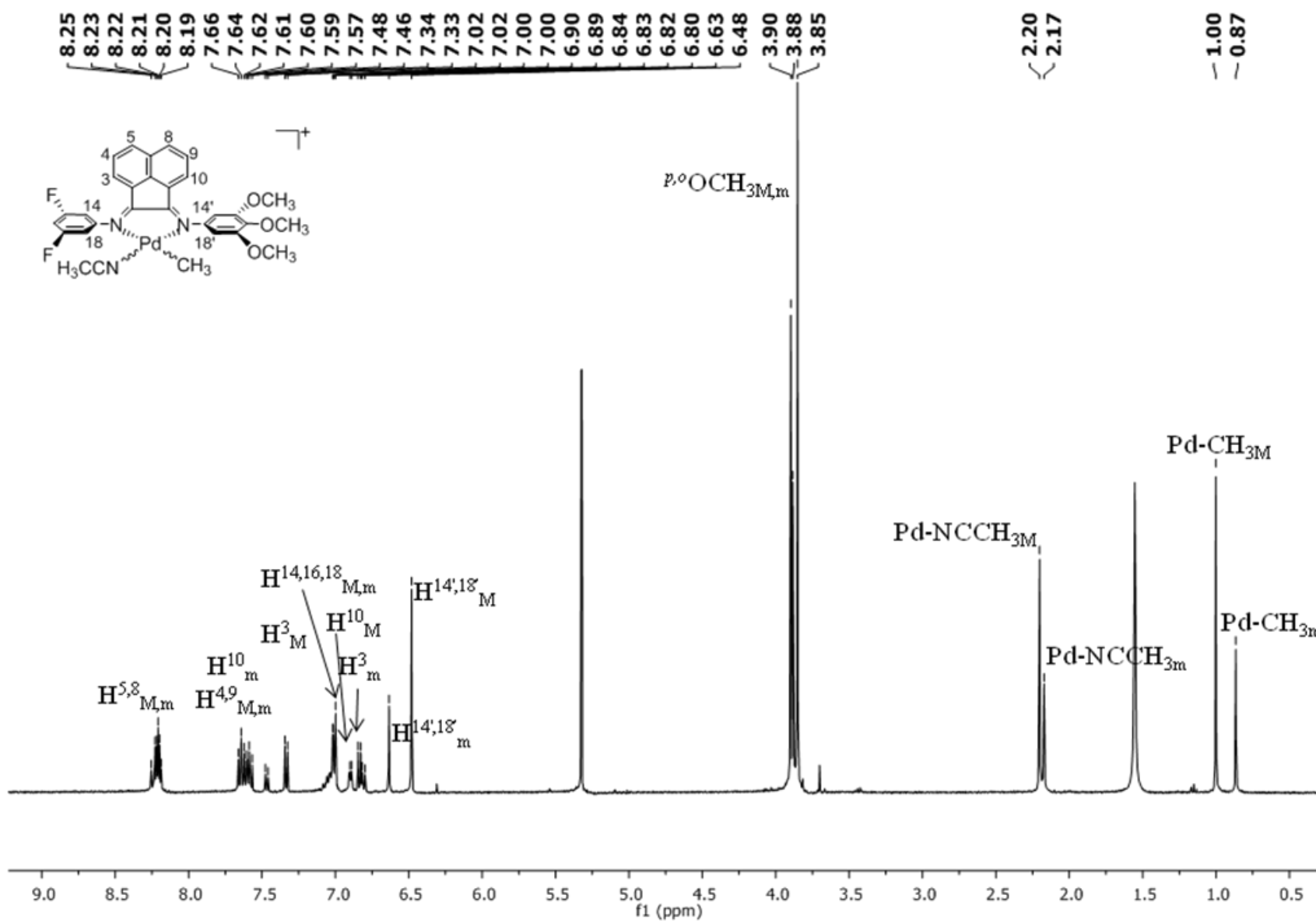


**Figure S32.**  $^1\text{H}$  NMR spectrum of complex **7b** ( $\text{CD}_2\text{Cl}_2$ , 500 MHz, 298 K).

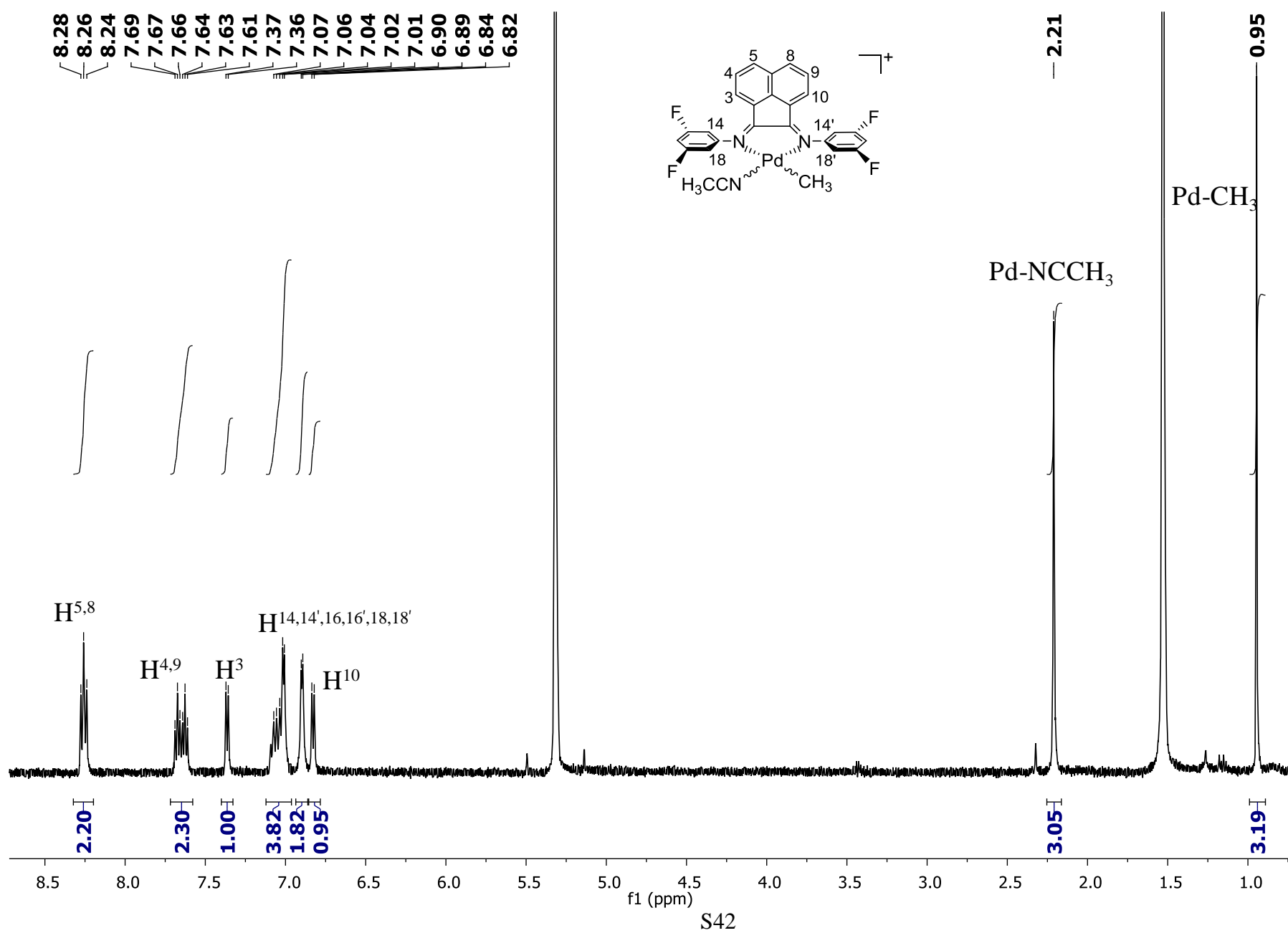


**Figure S33.**  $^1\text{H}$  NMR spectrum of complex **1c** ( $\text{CD}_2\text{Cl}_2$ , 200 MHz, 298 K).

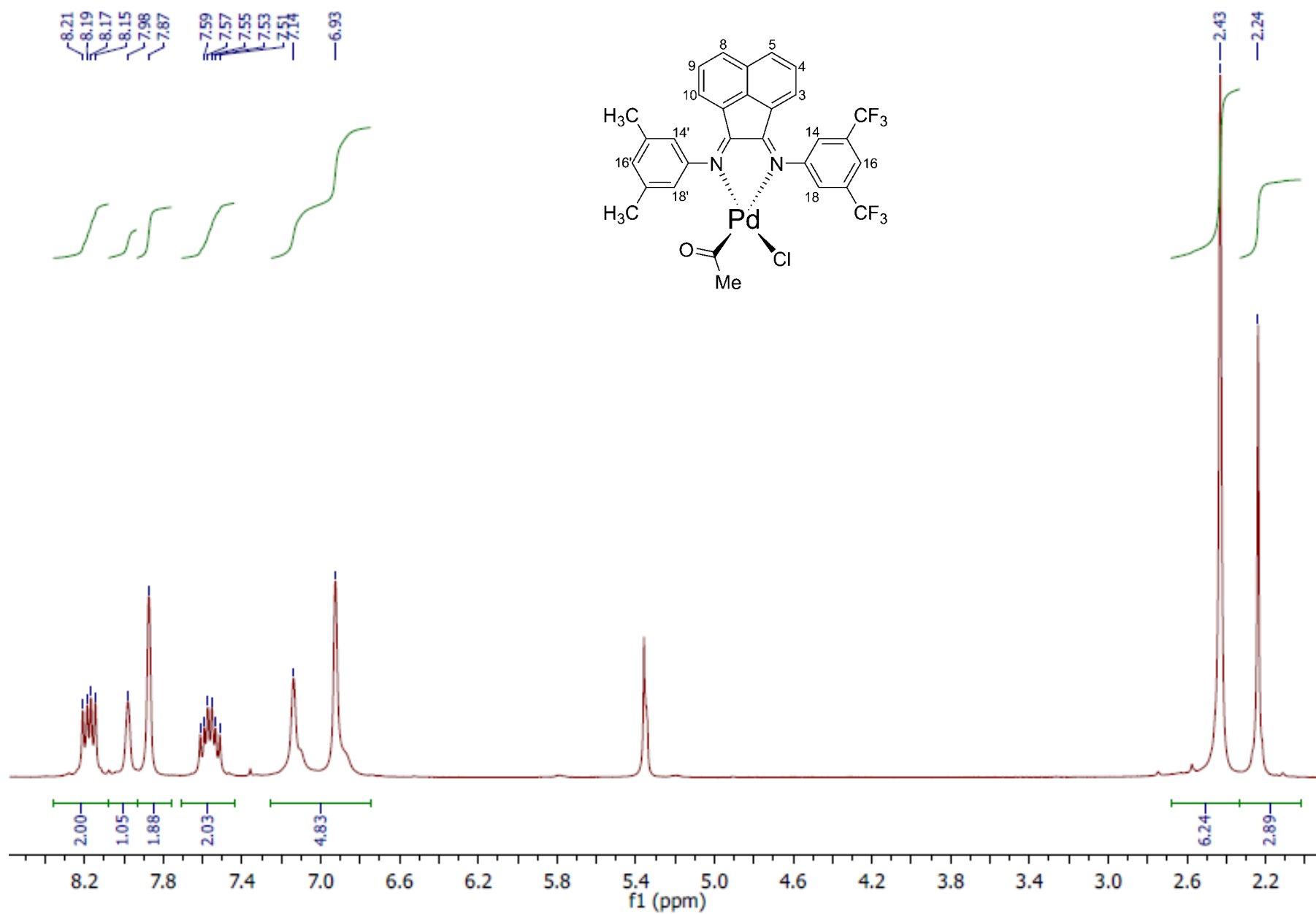


**Figure S34.**  $^{13}\text{C}$  NMR spectrum of complex **1c** ( $\text{CDCl}_3$ , 50 MHz, 298 K).

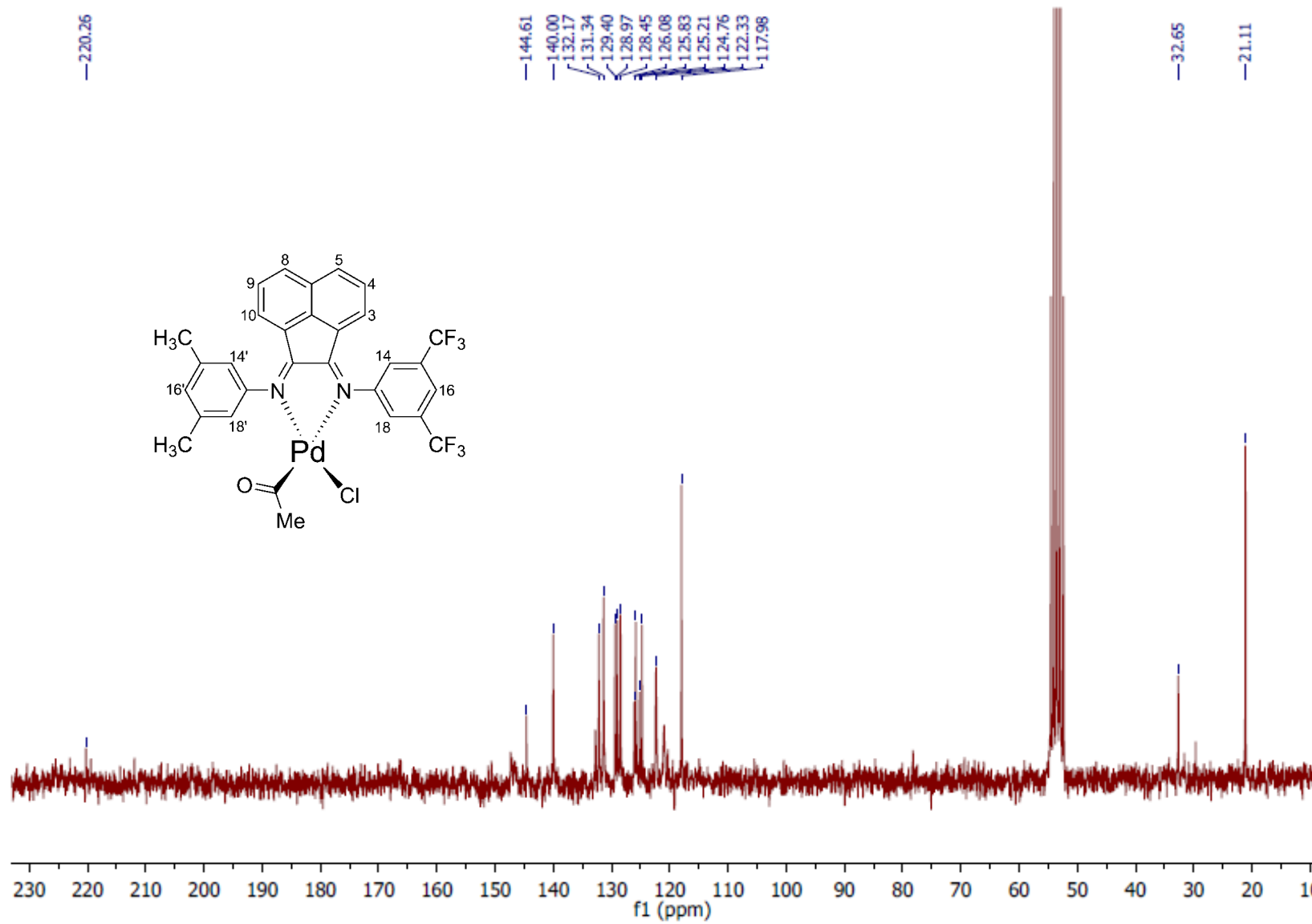


**Figure S35.**  $^1\text{H}$  NMR spectrum of intermediate **1d** ( $\text{CDCl}_3$ , 200 MHz, 298 K)

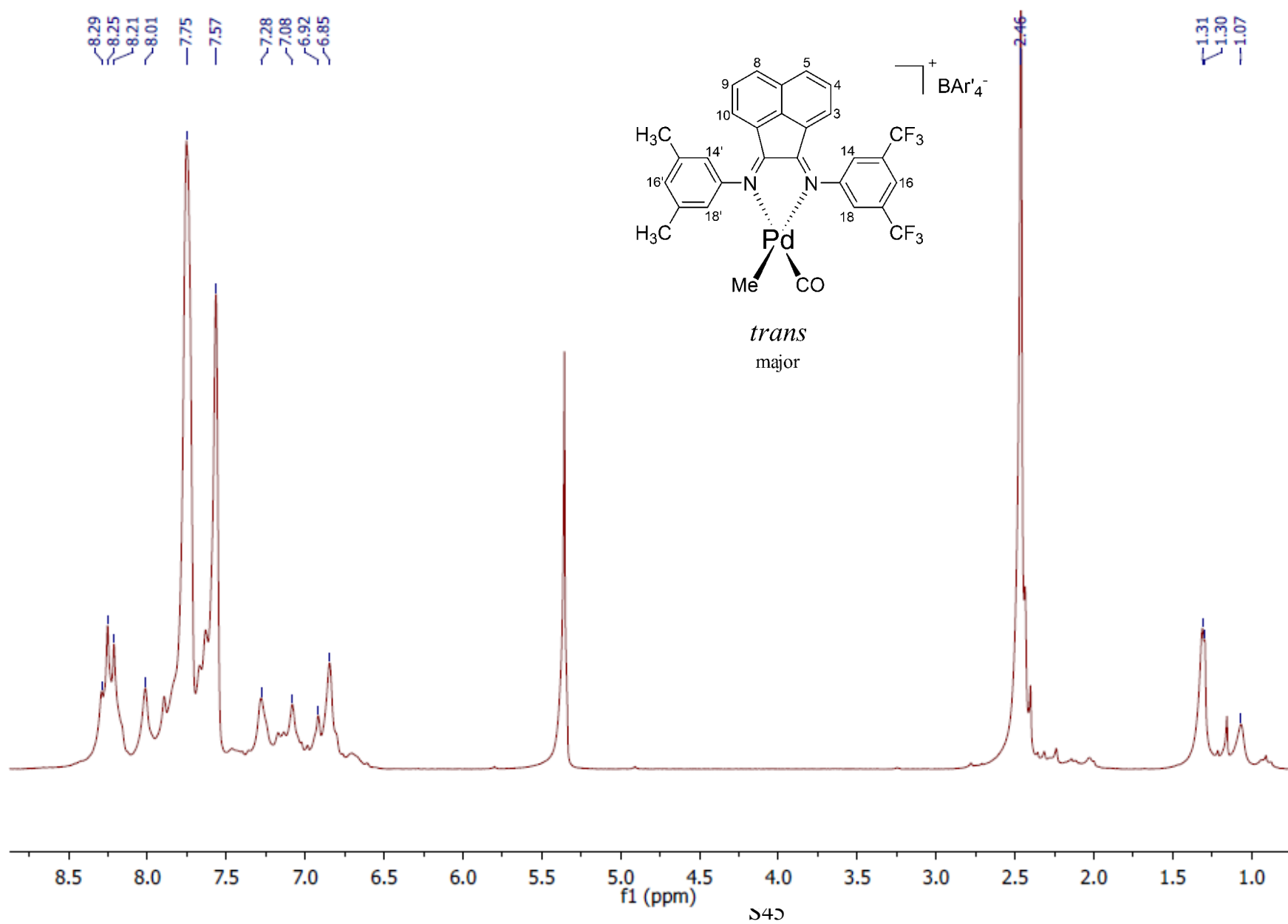


**Figure S36.**  $^{13}\text{C}$  NMR spectrum of intermediate **1d** ( $\text{CDCl}_3$ , 50 MHz, 245 K).

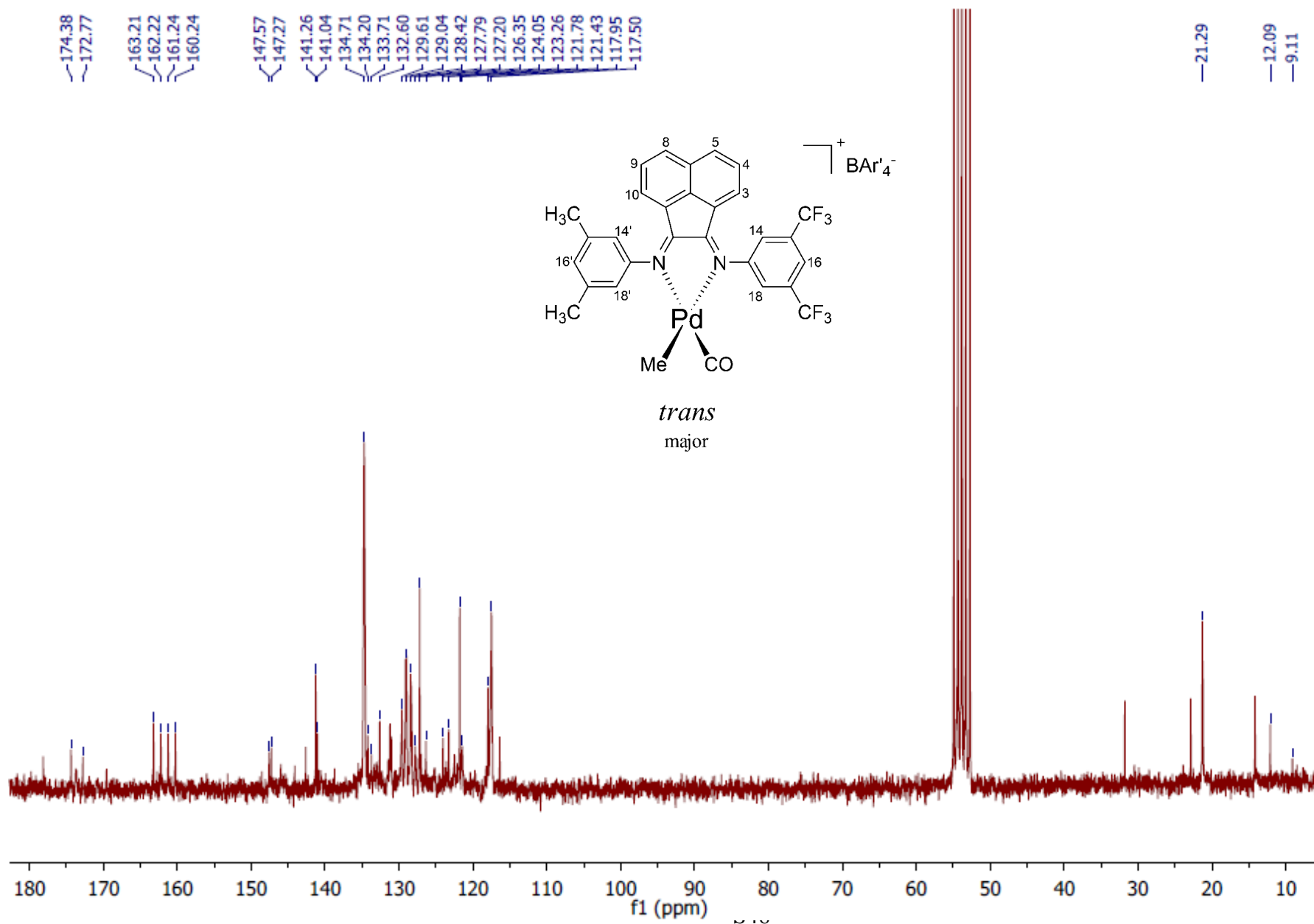


**Figure S37.**  $^1\text{H}$  NMR spectrum of intermediate **1e** ( $\text{CDCl}_3$ , 200 MHz, 298 K).

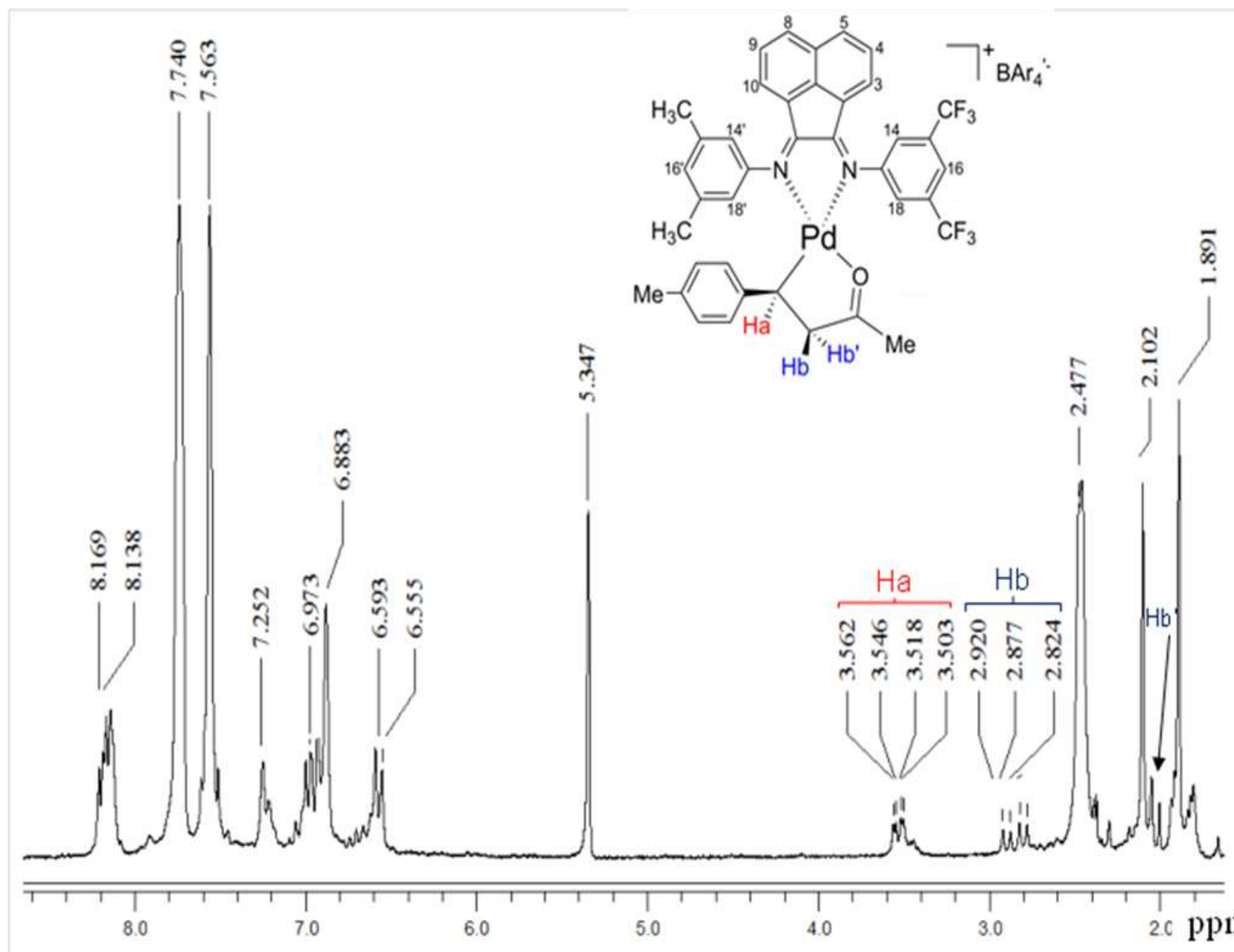


**Figure S38.**  $^1\text{H}$  NMR spectrum of intermediate **1f** ( $\text{CDCl}_3$ , 200 MHz, 253 K).

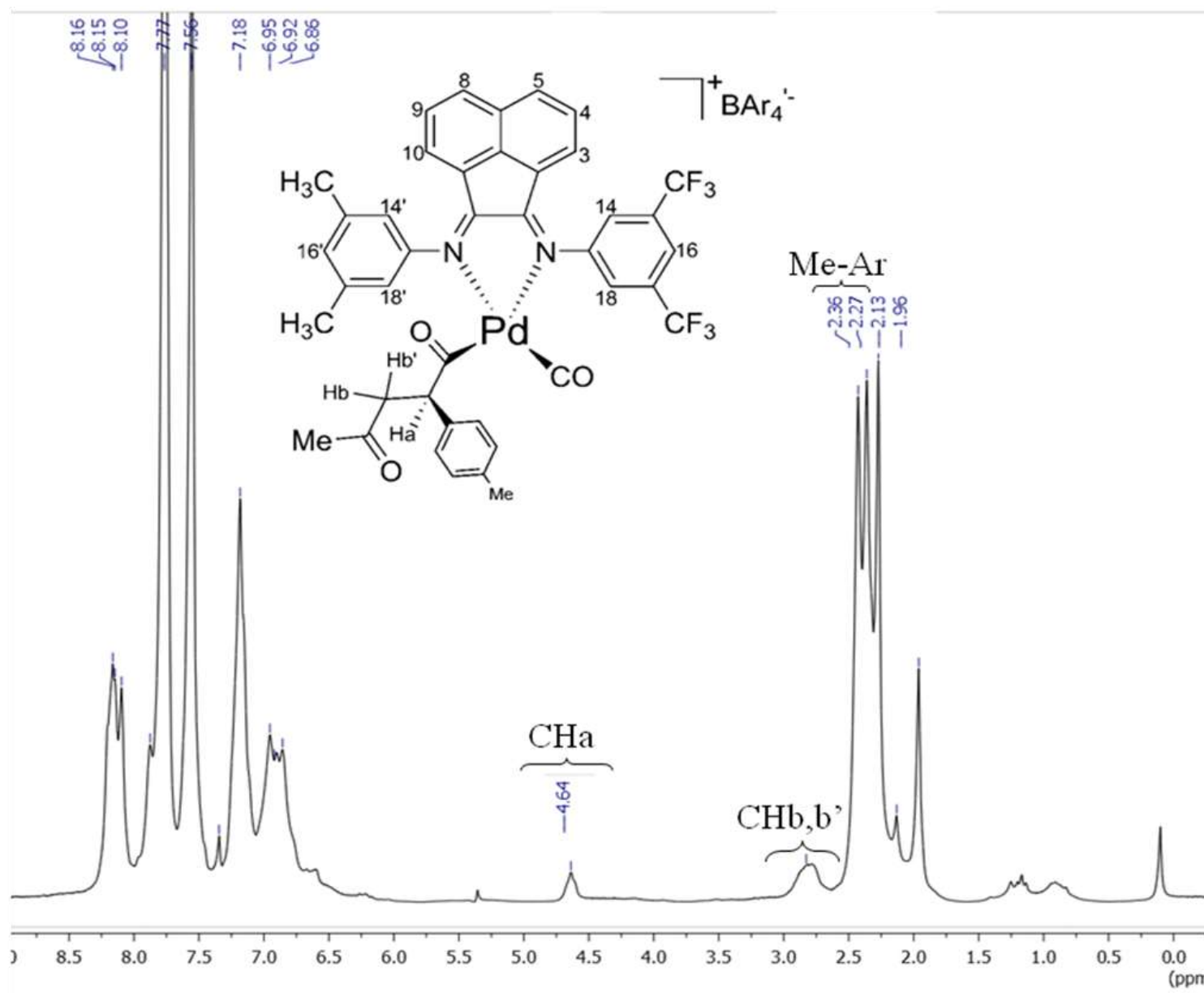
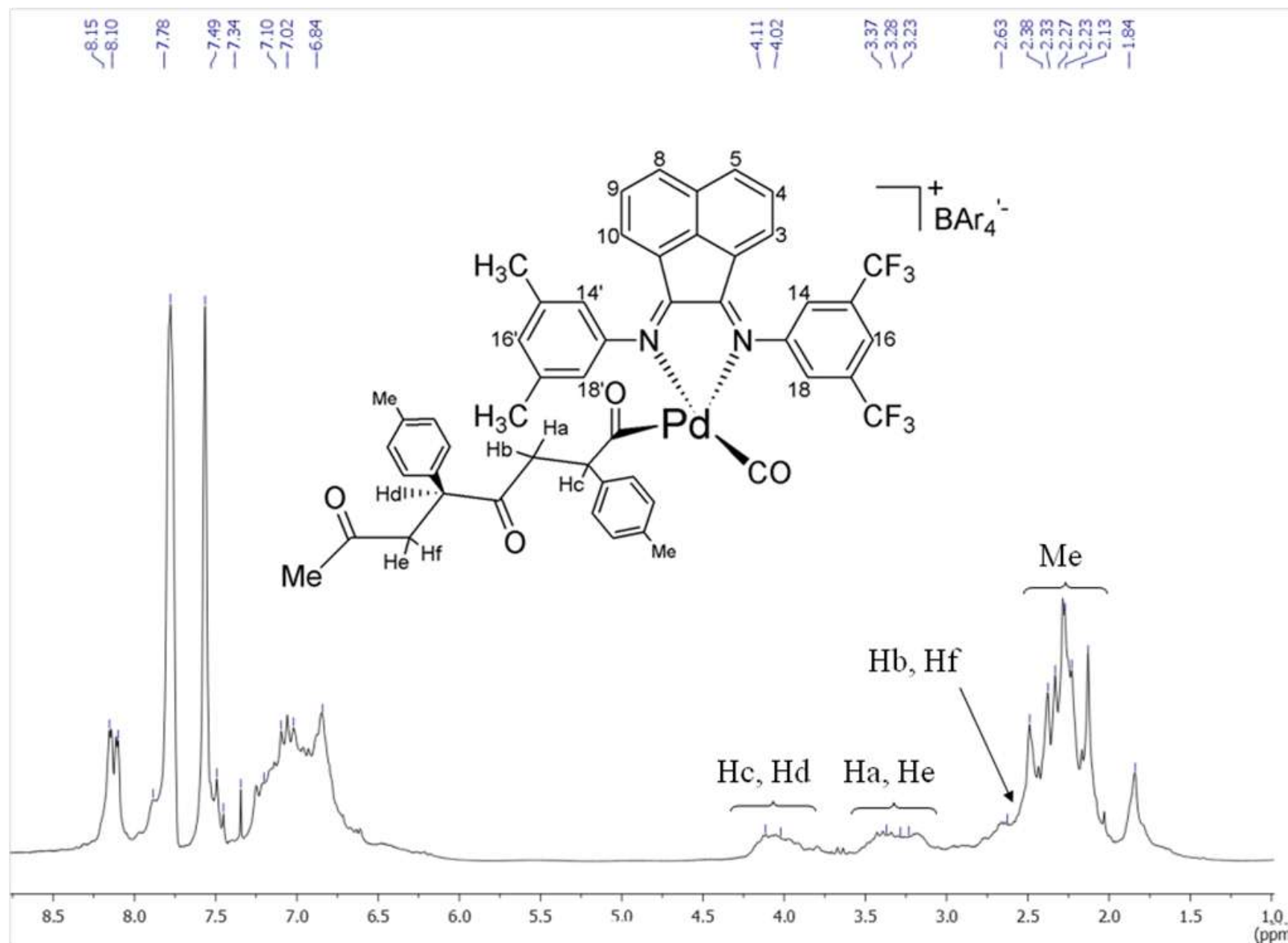


**Figure S39.**  $^1\text{H}$  NMR spectrum of intermediate **1g** ( $\text{CDCl}_3$ , 200 MHz, 243 K).





## References

1. C. Besson, E. E. Finney and R. G. Finke, *J. Am. Chem. Soc.*, 2005, **127**, 8179-8184.
2. M. A. Watzky and R. G. Finke, *J. Am. Chem. Soc.*, 1997, **119**, 10382-10400.
3. P. H. M. Budzelaar, P. W. N. M. Van Leeuwen, C. F. Roobek and A. G. Orpen, *Organometallics*, 1992, **11**, 23-25.
4. M. Tromp, J. R. A. Sietsma, J. A. van Bokhoven, G. P. F. van Strijdonck, R. J. van Haaren, A. M. J. van der Eerden, P. W. N. M. van Leeuwen and D. C. Koningsberger, *Chem. Commun.*, 2003, 128-129.
5. M. Portnoy, F. Frolow and D. Milstein, *Organometallics*, 1991, **10**, 3960-3962.
6. F. Ragagni, H. Larici, M. Rimoldi, A. Caselli, F. Ferretti, P. Macchi and N. Casati, *Organometallics*, 2011, **30**, 2385-2393.
7. M. Gasperini, F. Ragagni and S. Cenini, *Organometallics*, 2002, **21**, 2950-2957.
8. M. Gasperini and F. Ragagni, *Organometallics*, 2004, **23**, 995-1001.
9. M. Gasperini, F. Ragagni, E. Gazzola, A. Caselli and P. Macchi, *Dalton Trans.*, 2004, 3376-3382.
10. A. Scarel, M. R. Axet, F. Amoroso, F. Ragagni, C. J. Elsevier, A. Holuigue, C. Carfagna, L. Mosca and B. Milani, *Organometallics*, 2008, **27**, 1486-1494.
11. Note that the same "volume" amount of the two olefins was employed. Given the higher MW and molar volume of the methyl-substituted substrate, the molar concentration of the latter was actually a little lower than that of styrene during the reactions. However, the reactivity difference is much larger than that attributable to such a small dilution effect and must have a different origin.
12. M. Brookhart, M. I. Wagner, G. G. A. Balavoine and H. A. Haddou, *J. Am. Chem. Soc.*, 1994, **116**, 3641-3642.
13. S. Bartolini, C. Carfagna and A. Musco, *Macromol. Rapid Commun.* 1995, **16**, 9-14.
14. C. Carfagna, G. Gatti, D. Martini and C. Pettinari, *Organometallics*, 2001, **20**, 2175-2182.
15. A. Scarel, B. Milani, E. Zangrandi, M. Stener, S. Furlan, G. Fronzoni, G. Mestroni, S. Gladiali, C. Carfagna and L. Mosca, *Organometallics*, 2004, **23**, 5593-5605.
16. The experiment at 10 bar with 3,5-(CH<sub>3</sub>)<sub>2</sub>C<sub>6</sub>H<sub>3</sub>;3,5-(CF<sub>3</sub>)<sub>2</sub>C<sub>6</sub>H<sub>3</sub>-BIAN was also performed. It is not included in the discussion because the data are of poor quality. However, even if quantitative data are inaccurate, the reaction rate was without doubt slower than that of both the reactions run under 3 and 5 bar with the same ligand.